CHAPTER

Magnetoliposomes for dual cancer therapy

11

Ana Rita O. Rodrigues[1], Bernardo G. Almeida[1], João P. Araújo[2], Maria-João R.P. Queiroz[1], Paulo J.G. Coutinho[1] and Elisabete M.S. Castanheira[1]

[1]Centro de Química, Universidade do Minho, Braga, Portugal [2]IFIMUP/IN - Instituto de Nanociência e Nanotecnologia, Universidade do Porto, Portugal

CHAPTER OUTLINE

11.1 INTRODUCTION

Currently, cancer is one of the diseases with the highest incidence among the world population and a huge mortality rate. According to *World Cancer Research Fund International*, there were an estimated 14.1 million cancer cases around the world in 2012 and this number is expected to increase to 24 million by 2035. The main obstacles in the fight against cancer are due to the difficulties in early diagnosis, the cytotoxicity associated with antitumor drugs used in conventional

Inorganic Frameworks as Smart Nanomedicines. DOI: http://dx.doi.org/10.1016/B978-0-12-813661-4.00011-0

chemotherapy, and the lack of more efficient therapies. The pharmaceutical industry has successfully developed many potent chemotherapeutic agents. However, most of these active molecules are toxic and cause systemic toxicity (Kuznetsov et al., 1997, 1999). Therefore, the anticancer drug dosage used in chemotherapy is often selected by how much a patient can physically withstand, rather than by how much is needed for treatment. Typically, in conventional chemotherapy less than 0.1% of the drugs are taken up by tumor cells and the remaining 99.9% attack healthy tissues, making the efficiency of treatment compromised from the outset (Reszka et al., 1997; Perry, 2001; van der Veldt et al., 2010).

Regarding cytotoxicity problems, new therapeutic approaches are emerging that intend to allow a safer use of promising and powerful anticancer drugs. Magnetically-guided transport of biologically active substances, to target specific sites in human body, has been a focus of research in recent years. The ability to guide transported drugs and focus the active molecules to specific sites in the body can overcome systemic toxicity problems (Fig. 11.1), also allowing lower drug dosages and a more efficient treatment, not only in cancer but also in other diseases.

Concerning the ability to target specific sites of interest, magnetic nanoparticles have been widely investigated for magnetically-guided transport. Magnetic

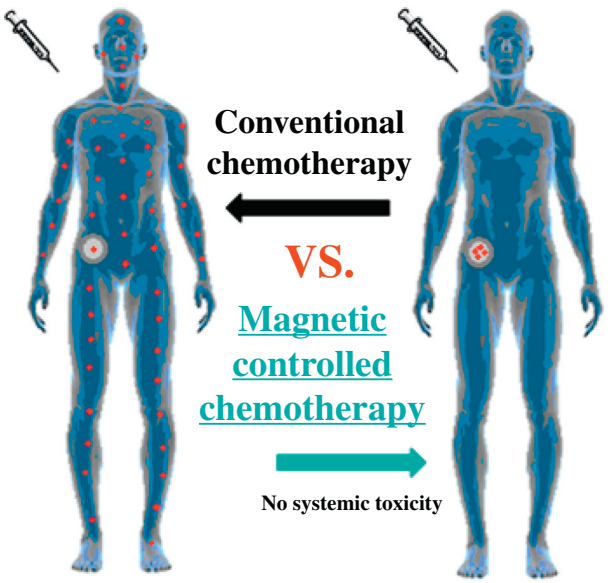

FIGURE 11.1

Schematic comparison between conventional chemotherapy and magnetic controlled chemotherapy.

nanoparticles offer major advantages due to their unique size, and physicochemical and magnetic properties, making them suitable to be guided and localized to therapeutic sites by external magnetic field gradients (Lubbe et al., 1999; Dandamudi and Campbell, 2007).

At sizes below 20−30 nm (depending on the materials), magnetic nanoparticles exhibit superparamagnetic behavior at room temperature (Baumgartner et al., 2013), which is preferred for biomedical applications. Superparamagnetism is a type of magnetism that occurs in small ferromagnetic or ferrimagnetic nanoparticles and is characterized by a very large magnetic moment only in the presence of an external magnetic field. When the external magnetic field is removed, there is no remnant magnetization and the net moment of the particles is randomized to zero (Cullity, 1972).

Superparamagnetism occurs in single-domain nanoparticles, i.e., nanoparticles that are composed by a single magnetic domain (a region within a magnetic material where the magnetization occurs in uniform direction), allowing the magnetization of nanoparticles to be approximated as one giant magnetic moment, by summing the individual magnetic moments (μ) of each constituent atom. This approximation, called the "macro-spin approximation," is responsible for the strong magnetic moment in the superparamagnetic nanoparticles. For single-domain nanoparticles, the energy required to invert the magnetization over the energy barrier from one stable magnetic configuration to another is related to $K_\mu V/kT$, where K_μ is the effective anisotropy constant, V the particle volume, k the Boltzmann's constant, and T the absolute temperature. Decreasing the particle size, the anisotropic energy ($K_\mu V$) decreases until the thermal energy (kT) causes fluctuations of the whole magnetic moments. In this situation, thermal fluctuations can affect the orientation of magnetization if they are large enough to overcome the magnetic anisotropy barrier. For ferromagnetic materials, the magnetic anisotropic energy is much larger than thermal energy (kT) (Fig. 11.2 (blue line)).

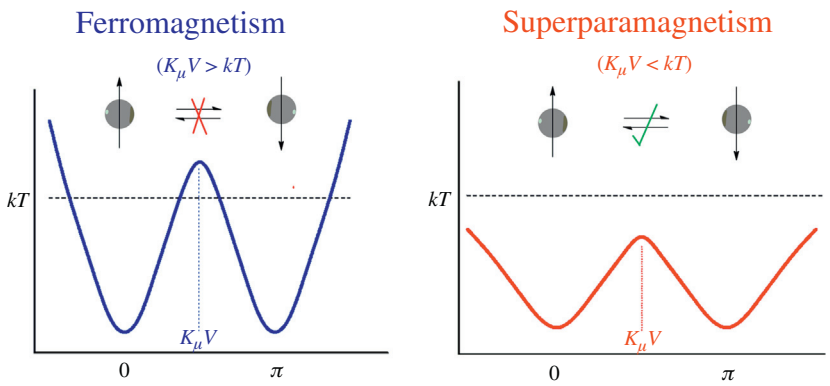

FIGURE 11.2

Nanoscale transition of magnetic nanoparticles from ferromagnetism to superparamagnetism; energy diagram of magnetic nanoparticles.

However, when nanoparticles are small enough for thermal energy to overcome the anisotropy energy ($K_\mu V$), the magnetization is no longer stable and the particle becomes superparamagnetic (Fig. 11.2 (red line)). Therefore, the magnetic moment can be easily saturated in the presence of an applied field, but upon field removal, magnetization returns to zero due to the thermal fluctuations (Altavilla and Ciliberto, 2011). This type of magnetic nanoparticle is characterized by the absence of hysteresis, coercivity, and remnant magnetization at room temperature.

For biomedicine, magnetic nanoparticles with superparamagnetic behavior are ideal, as they exhibit a strong magnetization, but only in presence of an external magnetic field (Dandamudi and Campbell, 2007; Gregoriadis, 1995; Markides et al., 2012). Further requirements are important for biomedical applications, such as their stability at pH = 7 and in physiological environment. Moreover, to prevent changes from the original structure, biodegradation in the biological environment and the formation of large aggregates and sediments, which could be a safety concern, magnetic nanoparticles should be encapsulated (Medeiros et al., 2011; Akbarzadeh et al., 2012).

Many coating systems, such as liposomes (Pradhan et al., 2010), polymers (Li et al., 2011), and hydrogels (Mitsumata et al., 2012) have been studied. Liposomes are nano-sized vesicles made of natural and nontoxic molecules. This nanoencapsulation system is biologically inert, weakly immunogenic, and has been described as an ideal drug delivery system (Poste et al., 1982; Mezei and Gulasekharam, 1982; Juliano, 1981). It can overcome many of the problems associated with other systems used in therapy, such as those involving solubility, pharmacokinetics, in vivo stability, and toxicity (Andresen et al., 2005; Ochekpe et al., 2009). Furthermore, liposomes can encapsulate both lipophilic and hydrophilic molecules in their lipid bilayer and aqueous core, respectively. However, liposomes still present some issues for in vivo application, namely their recognition and capture by the immune system (Lubbe et al., 1999) and the location in therapeutic sites for drug release (Dandamudi and Campbell, 2007).

By combining the amazing physical properties of magnetic nanoparticles and liposomes, the individual limitations of both systems for in vivo application are overwhelmed. When entrapping magnetic nanoparticles in liposomes, the magnetic properties of the former are preserved (Bulte et al., 1999). The term "magnetoliposome" was first introduced by De Cuyper and coworkers (De Cuyper and Joniau, 1988) to describe structures where the interior of the phospholipid vesicle was entirely packed with magnetic nanoparticles. The so-called magnetoliposomes are of great importance as they can be used in an array of biomedical applications. In therapy, the most promising applications of these magnetic-sensitive liposomes are magnetic controlled drug delivery and hyperthermia (Nuytten et al., 2010; Tromsdorf et al., 2007). These magnetic nanoparticle-based systems are highly differentiated from other nanosystems used in current therapies, as they can provide a dual therapeutic approach, by combining synergistic magnetic hyperthermia and chemotherapy capabilities in a single bionanosystem,

improving treatment from the start. Conversely, in diagnosis, magnetic nanoparticles have been used as contrast agents in magnetic resonance imaging (MRI) (Weinmann et al., 2003).

11.2 MAGNETIC NANOPARTICLES: SYNTHESIS AND CHARACTERIZATION

The synthesis method for the preparation of magnetic nanoparticles is of extreme importance, as the final magnetic and physicochemical properties, such as size distribution, shape, and surface chemistry, depend on its choice. The preparation method determines the structural degree of defects or impurities in the particles, as well as the distribution of such defects and, consequently, their magnetic properties (Perez et al., 1997; Lee et al., 2005; Sjogren et al., 1997; Akbarzadeh et al., 2012).

Several techniques for the synthesis of magnetic nanoparticles have been developed to yield monodisperse colloids, consisting of uniform nanoparticles both in size and shape, and to achieve a proper control of crystallinity and magnetic properties (Teja and Koh, 2009), in which the entire uniform physicochemical properties directly reflect the properties of single particles (Bao et al., 2006). To date, many preparation methods have been reported, including coprecipitation, microemulsion, thermal decomposition, solvothermal technique, chemical vapor deposition, combustion synthesis, and others (Akbarzadeh et al., 2012). Among them all, coprecipitation is the most used method and the most appropriate for great size distributions and good magnetic properties (Kumar, 2013). It has been extensively employed for biomedical applications as it is the simplest and most efficient chemical pathway (Laurent et al., 2008). It also does not require harmful materials or procedures, being cost-effective (Indira and Lakshmi, 2010).

As previously mentioned, superparamagnetic nanoparticles are preferred in biomedicine. When using this type of nanoparticles, typical assessments must be done in order to confirm that the proper chemical and magnetic properties are accomplished. The particles size and polydispersity have to be evaluated; the superparamagnetic behavior depends on the crystallite size and occurs below typical critical diameters, depending on the material. The crystalline structure of the samples may also give relevant information about the magnetic behavior, as magnetic properties strongly depend on the distribution of ions among the crystallographic lattice sites. The characteristics of any magnetic material are important as well, and are best described in terms of their magnetization dependence on the applied field, the so-called hysteresis loop. This is the most common measurement used to evaluate the magnetic parameters and is performed by fixing the temperature and measuring the magnetization at a series of different applied magnetic fields. This type of measurement gives information about the maximum magnetization, the degree at which the sample remains magnetized when the

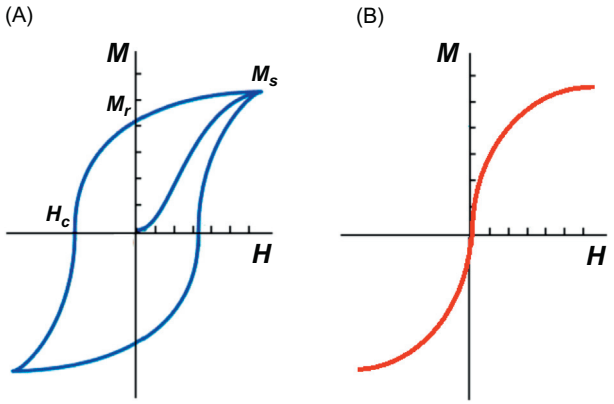

FIGURE 11.3

Schematic illustration of (A) a typical hysteresis loop of an array of single-domain ferromagnetic nanoparticles and (B) a typical curve for a superparamagnetic material.

applied field is removed, the so-called remnant magnetization (M_r), and how easily the sample magnetization can be reversed, the coercive field (H_c). In this type of measurement, the application of a sufficiently large external magnetic field causes the spins of the material to align with the field until the maximum value of magnetization is achieved (all spins aligned), this state being the saturation magnetization, M_s. The external magnetic field then decreases until zero magnitude, the spins cease to be aligned with the field, and the total magnetization decreases. For a ferromagnetic material, a residual magnetic moment and coercive field are observed at zero field (Fig. 11.3A), whereas, for a superparamagnetic material, these values tend to zero (Fig. 11.3B).

The ratio between the remnant magnetization and the saturation magnetization, M_r/M_s, is called the magnetic squareness value and varies from 0 to 1 (Mathew and Juang, 2007), representing the loss of more than 90% of the magnetism upon removal of the applied magnetic field (Mathew and Juang, 2007; Schulz et al., 2009; Khanna and Verma, 2013a,b). The presence of superparamagnetic behavior can be related to this ratio value, being of the order or below 0.1 for a superparamagnetic material. High saturation magnetization and low coercivity values are ideal for superparamagnetic nanoparticles in biomedical applications. With high magnetization values, the magnetic nanoparticles can be easily controlled by the presence of an external magnetic field. Moreover, the inductive heating property of nanoparticles, under an alternate magnetic field, is inversely related to the coercive field and directly proportional to the saturation magnetization (Li-Ying et al., 2010).

The temperature dependence of the magnetization is also an important parameter. The magnetic response to an applied magnetic field at a given temperature is

not always the same and depends on whether the sample has been cooled with an applied magnetic field or without. This measurement consists of two curves, the zero-field cooled (ZFC) and the field cooled (FC). The curves are obtained by initially cooling the sample under an applied magnetic field of $H \sim 100$ Oe (FC) and then the magnetization is measured with increasing temperature (applied field of $H \sim 50$ Oe). Subsequently, after reaching the maximum temperature, the sample is recooled, now without any applied magnetic field (ZFC). The magnetization is measured with increasing temperature, under the same magnetic field of $H \sim 50$ Oe. As temperature increases, the blocked magnetic moments align with the applied field, leading to an initial increase of the sample magnetization. However, as soon as thermal fluctuations allow the moments to overcome the magnetic anisotropy energy barrier, the thermal randomization of the intraparticle magnetic moments produces a subsequent decrease of the magnetization curve, with increasing temperature. In this way, the ZFC curve peak corresponds to the sample blocking temperature, T_B, above which the material becomes superparamagnetic. Typically, above the blocking temperature, the ZFC and the FC curves coincide. This occurs because the system is in thermal equilibrium. For temperatures below the blocking temperature, in the field cooling curve, the moment remains partially aligned with the applied magnetic field, and so the magnetic moment of the sample does not tend to zero (Sattler, 2010).

11.2.1 IRON OXIDE–BASED NANOPARTICLES

Iron oxide–based nanoparticles have attracted a great deal of interest in biomedical research over the past decades, due to their superparamagnetic properties, high biocompatibility, and nontoxicity (Mahmoudi et al., 2011). Iron oxide–based nanoparticles consist of iron, oxygen, and/or OH groups, but differ in the valence of iron and on the overall crystalline structure. They can be oxides, hydroxides, and oxide-hydroxides, and can be easily synthesized in laboratory. The main forms of iron oxide–based nanoparticles with biological interest are magnetite (Fe_3O_4) and its partially oxidized form maghemite (γ-Fe_2O_3) (Fernández-Remolar, 2014).

The structure of magnetite is a face-centered cubic inverse spinel, consisting of a cubic close-packed array of oxide ions, where all Fe^{2+} ions occupy half of the octahedral sites and the Fe^{3+} ions split evenly across the remaining octahedral and tetrahedral sites. Coupling between magnetic moments of the iron moieties located at tetrahedral and octahedral sites results in a ferromagnetic ordering in bulk. The maghemite structure is a cubic defect spinel, similar to that of magnetite, but with vacancies in the cation sublattice. Oxygen anions give rise to a cubic close-packed array, while Fe^{2+} ions are distributed over tetrahedral sites and octahedral sites. The resulting magnetic behavior is ferrimagnetic. At nanoscale, magnetite and maghemite present distinct magnetic behaviors when compared to those of the bulk materials. Namely, an assembly of noninteracting magnetite

nanoparticles exhibits superparamagnetism at high temperatures and ferromagnetic (ferrimagnetic for maghemite) behavior below the blocking temperature, T_B.

Iron oxide–based nanoparticles, either magnetite (Fe_3O_4) or maghemite (γ-Fe_2O_3), can be easily obtained by a coprecipitation method, an aging stoichiometric mixture of ferrous and ferric salts in aqueous medium. The chemical reaction of magnetite formation may be written as Eq. (11.1). According to thermodynamics, complete precipitation should be expected at pH values between 8 and 14, with a stoichiometric ratio (Fe^{3+}:Fe^{2+}) of 2:1 in a nonoxidizing oxygen environment (Laurent et al., 2008; Meledandri et al., 2011).

$$Fe^{2+} + 2Fe^{3+} + 8OH^- \rightarrow Fe_3O_4 + 4H_2O \tag{11.1}$$

However, magnetite is not very stable and is sensitive to oxidation, being transformed into maghemite in the presence of oxygen, as described by Eq. (11.2):

$$Fe_3O_4 + 2H^+ \rightarrow \gamma - Fe_2O_3 + Fe^{2+} + H_2O \tag{11.2}$$

The influence of different factors on the magnetic properties and size distribution of iron oxide nanoparticles has been widely studied. Modulating different parameters, such as Fe^{2+}/Fe^{3+} ratio, nature of salts (perchlorates, chlorides, sulfates, and nitrates) and bases (ammonia, CH_3NH_2, and NaOH), it is possible to obtain nanoparticles with a size range from 4.2 to 16.6 nm (Babes et al., 1999; Gribanov et al., 1990; Jolivet et al., 2014). Magnetite nanoparticles obtained by the coprecipitation of Fe^{2+} and Fe^{3+} salts, with a stoichiometric ratio of 2:1 (Fe^{3+}/Fe^{2+}), using sodium hydroxide as motor of the reaction and in an oxygen-free environment, exhibit a spherical form and uniform size, with diameters $\sim$12 nm (Fig. 11.4A). Moreover, these nanoparticles exhibit superparamagnetic properties at room temperature, with saturation magnetization $\sim$60 emu/g, a coercive field of 9.7 Oe (Fig. 11.4B), and a blocking temperature of 118 K. The low coercive field and the reasonable saturation magnetization of the synthesized Fe_3O_4 nanoparticles indicate that they can be suitable for hyperthermia therapy. Published results reported coercivity values of near zero for magnetite nanoparticles of 8 nm size, while for nanoparticles of 12 nm diameter, a coercivity of 18 Oe was observed (Li-Ying et al., 2010; Lu et al., 2010). It was also shown that Fe_3O_4 nanoparticles with 16 nm and a coercive field of 27 Oe were able to produce heat with high efficiency in hyperthermia applications (Li-Ying et al., 2010).

The variation of a few parameters in the coprecipitation method, such as the flux rate or the order of salts addition, causes different sizes and structures for the magnetite nanoparticles. The modulation of acidity and ionic strength of the synthesis media enables the tailoring of nanoparticles with sizes in the range of 2–15 nm; shape variations can be related to modification of electrostatic surface

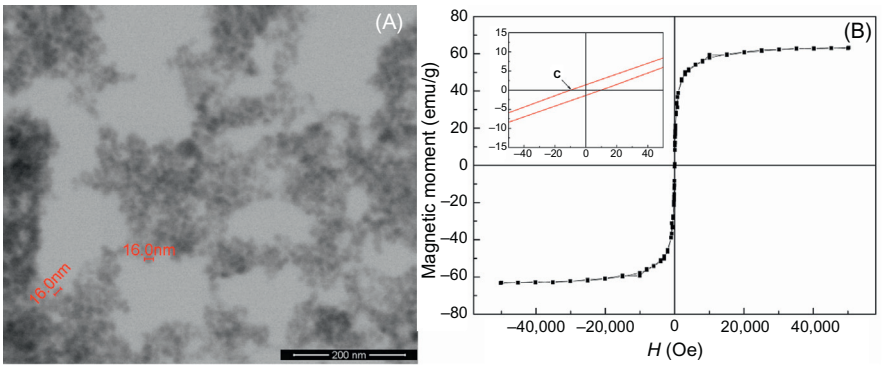

FIGURE 11.4

(A) SEM image of magnetite nanoparticles prepared by coprecipitation method in aqueous solution. (B) Hysteresis cycle of magnetite nanoparticles at room temperature. Inset: Enlargement of the cycle in the low field region, with indication of the coercive field (c).

density of the nanoparticles (Jolivet et al., 1997; Jolivet and Chaeneac, 2002; Massart and Cabuil, 1987).

The major difficulty related to the coprecipitation method is the control of crystal growth. The microemulsion (water in oil) method makes use of water droplets as nanoreactors to control size distribution (Inouye et al., 1982; Muller and Muller, 1984; Gupta and Wells, 2004). In this method, iron precursors can be precipitated in water pools of reverse micelles. Iron oxides do not precipitate in the organic phase, as the iron precursors are unreactive in this phase. The size of nanoparticles can be controlled by regulating the size of the water droplets and surfactants can be used for the particle dispersion. The preparation of iron oxide nanoparticles by thermal decomposition of iron carboxylate salts has significantly improved the quality of traditional nanoparticles in terms of size tunability, monodispersity, and crystalline structure (Mahmoudi et al., 2011).

11.2.2 TRANSITION METAL FERRITES

Despite the great physicochemical, magnetic properties, and biocompatibility of iron oxide–based nanoparticles, they become less desirable because the iron atoms are poorly distinguishable from those of hemoglobin (Sharifi et al., 2012). Alternatively, an increasing interest has been devoted to the development of transition metal ferrites (MFe_2O_4, M = Mn, Ni, Co, Zn), with enhanced magnetic properties and strong interest for biomedical applications. These nanoparticles are remarkably soft-magnetic with superparamagnetic behavior and possess great properties, such as high saturation magnetization, good chemical stability, and

high biocompatibility (Pereira et al., 2012; Carta et al., 2010). Transition metal ferrites have spinel structure, with a cubic close-packed arrangement of oxygen atoms, with M^{2+} and Fe^{3+} in two different crystallographic sites. The spinel structure contains two cation sites for metal cation occupancy. There are eight tetrahedral sites in which the metal cations are tetrahedrally coordinated with oxygen, and 16 octahedral sites which possess octahedral coordination. Magnetically, spinel ferrites display ferrimagnetic ordering and their electrical and magnetic properties depend upon the choice of cation and its distribution between tetrahedral and octahedral sites in the spinel lattice. This is highly sensitive to preparation methods, annealing temperature, chemical composition, and nature of dopants (Mathew and Juang, 2007; Vestal and Zhang, 2004).

Nickel ferrite nanoparticles ($NiFe_2O_4$) have been proposed as less cytotoxic for HeLa cells than cobalt ($CoFe_2O_4$) or zinc ferrite ($ZnFe_2O_4$), being more promising for biomedical applications (Tomitaka et al., 2009; Khanna and Verma, 2013a,b). In general, most of the methods proposed for the synthesis of nickel ferrite nanoparticles produce particles with low precise control over the size and distribution. However, a coprecipitation method promotes the synthesis of small nickel ferrite nanoparticles with superparamagnetic behavior and reasonable size distribution. $NiFe_2O_4$ nanoparticles can be easily synthesized by the reduction of salts with a stoichiometric ratio of 2:1 (Fe^{3+}/Ni^{2+}) and using sodium hydroxide, a calcination process being required to obtain a crystalline phase of nickel ferrite spinel (Rodrigues et al., 2015). Several studies reported that, as the annealing temperature increases, particles with higher saturation magnetization are formed. However, crystallite size and coercive and remnant fields also increase and the nanoparticles become nonsuperparamagnetic. In the case of nickel ferrite nanoparticles, the transition from a superparamagnetic to bulk magnetic behavior occurs at an annealing temperature of around 800°C (Gharagozlou, 2011; Malik et al., 2010).

Recently, small nickel ferrite nanoparticles with a size distribution of 11 ± 5 nm were obtained by coprecipitation method, followed by calcination at 800°C (Fig. 11.5). The magnetic squareness value of 7.2×10^{-5} indicates that the nanoparticles are superparamagnetic at room temperature, exhibiting a blocking temperature of $T_B \sim 214$ K and a coercivity field of 12 Oe (Rodrigues et al., 2015). Another study reports the synthesis of $NiFe_2O_4$ nanoparticles with a saturation magnetization value of 40 emu/g at room temperature, also using the coprecipitation method (Maaz et al., 2009).

Other preparation methods have been proposed for the synthesis of nickel ferrite nanoparticles suitable for biomedical applications, with superparamagnetic behavior at room temperature and with high saturation magnetization. Hydrothermal and sol−gel auto-combustion methods have yielded nickel ferrite nanoparticles with high saturation magnetizations of 39.60 emu/g (Nejati and Zabihi, 2012) and 50.4 emu/g (Sivakumar et al., 2011a,b). The magnetic nanoparticles obtained by hydrothermal method have sizes of 50−60 nm that decrease up

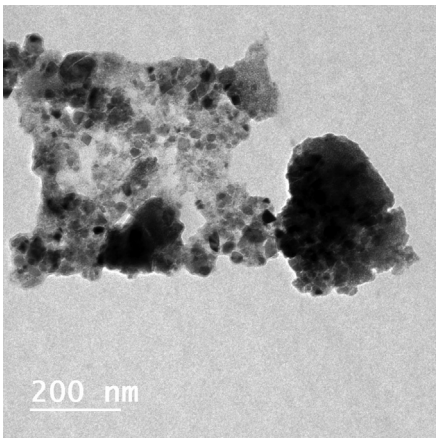

FIGURE 11.5

TEM image of $NiFe_2O_4$ nanoparticles synthesized by coprecipitation method and calcinated at 800°C.

to 10−15 nm in the presence of surfactants. The nanoparticles obtained via sol−gel auto-combustion process exhibit a spherical shape and an average size of 8 nm (Nejati and Zabihi, 2012; Sivakumar et al., 2011a,b).

Manganese ferrite nanoparticles have also received increased attention because of their higher magnetic susceptibility, comparing with other ferrite nanoparticles (Cabrera et al., 2012). Manganese ferrite nanoparticles have also shown good biocompatibility and slight toxicity against HeLa cells (Tomitaka et al., 2009). Due to their small sizes, manganese ferrite nanoparticles have been proposed as positive contrast agents for MRI. It is known that the surface atom ratio and the particle degradation rate are inverse to particle size. Larger particles exhibit lower surface Mn^{2+} ratio and slower release of Mn^{2+} than small ones, leading to a small longitudinal relaxivity. Therefore, reducing their size is considered an important strategy to improve longitudinal relaxivity, as observed for MnO colloids with 2−3 nm size (Li et al., 2013; Baek et al., 2010). Manganese ferrite nanoparticles have a partially inverse spinel structure, with about 80% of Mn^{2+} ions located at tetrahedral sites and only 20% of them located at octahedral sites (Deraz and Alarifi, 2012). The critical diameter, below which the particles possess superparamagnetism at room temperature, is 42.9 nm (Rafique et al., 2013).

The synthesis of manganese ferrite nanoparticles by the coprecipitation method stands out, again, as an economical and efficient chemical route for large-scale synthesis of superparamagnetic nanoparticles. Using stoichiometric ratio of 2:1 (Fe^{3+}/Mn^{2+}), pure crystalline manganese ferrite nanoparticles can be easily precipitated in aqueous solution with sodium hydroxide, without the need of calcination to obtain a crystalline structure. These particles are superparamagnetic at

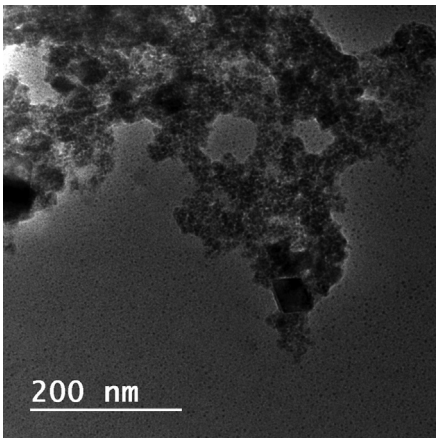

FIGURE 11.6

TEM image of $MnFe_2O_4$ nanoparticles synthesized by coprecipitation method and without calcination.

room temperature, exhibiting very small hysteresis and a coercive field of 6.3 Oe (Rodrigues et al., 2016). Samples with uniform shape and good size distribution, with sizes around or below tens of nanometers (Fig. 11.6), have been obtained by coprecipitation (Rodrigues et al., 2016; Zipare et al., 2015).

Other synthesis methods have yielded manganese ferrite nanoparticles with very good magnetic properties, including a high saturation magnetization of 69 emu/g (Zipare et al., 2015).

11.2.3 CALCIUM AND MAGNESIUM FERRITES

In the past few years, rising attention has been given to the synthesis of other ferrite nanoparticles, without transition metals in their constituents, due to the toxicity of metal ferrite nanoparticles. Ions such as Ca^{2+} and Mg^{2+} have been proposed to substitute those transition metals in the crystalline structure of ferrite nanoparticles, as they may promote a higher biocompatibility (Saldívar-Ramírez et al., 2014; Wan et al., 2008). Instead of causing injury, these ions are expected to be safely metabolized by the human body. Despite the biological potential of these nanoparticles, their toxicity towards cancer cells has not yet been deeply investigated. However, some studies show that magnesium ferrite nanoparticles possess less cytotoxic effects against human astrocytoma U87 cells (Lai et al., 2008). Concerning calcium ferrite nanoparticles, in vitro cytotoxicity tests on T-cell lines showed that these kinds of particles are biocompatible at concentrations below 250 mg/mL, exhibiting an enhanced cell viability when compared to other ferrites (Khanna and Verma, 2013a,b).

Magnesium ferrite nanopowders can be used as hyperthermia agents, as they display a high heating capacity, which generates appropriate temperatures for hyperthermia application (Maehara et al., 2005; Sato et al., 2008). Calcium ferrite nanoparticles are also promising for hyperthermia because of their high thermal stability, making them appropriate for a wide range of temperatures (Sulaiman et al., 2015). Likewise, mixed magnesium and calcium ferrite nanoparticles have also shown to be appropriate for hyperthermia-based therapies. A partial substitution of the Mg^{2+} sites by Ca^{2+} ($0.2 - 0.8$ in x of $Mg_{1-x}Ca_xFe_2O_4$) caused a rise in temperature up to 50°C in a sample of 1.0 g weight, using an AC magnetic field of 370 kHz and 1.77 kA/m (Hirazawa et al., 2008).

Magnesium ferrite nanoparticles are crystallized in a partially inverse structure, with Mg^{2+} ions mainly on octahedral sites, while Fe^{3+} ions are distributed almost equally among tetrahedral and octahedral sites (Bamzai et al., 2013). Among all the techniques available for the synthesis of magnesium ferrite nanoparticles, the most used are sol−gel, coprecipitation and combustion methods (Murugesan and Chandrasekaran, 2015; Kanagesan et al., 2013; Chandradass et al., 2012; Kaur and Kaur, 2014). Hirazawa and coworkers have reported crystal diameters of ∼37 nm for magnesium ferrite nanoparticles obtained by coprecipitation method (Hirazawa et al., 2008). In order to obtain smaller particles, reverse coprecipitation and reverse micelle methods have been proposed, to achieve nanoparticles with crystallite diameters of 15 and 12 nm, respectively (Aono et al., 2008; Chandradass et al., 2012). Considering the degree of magnetization, superparamagnetic magnesium ferrite nanoparticles (obtained by coprecipitation) have shown low saturation magnetization values, around or lower than 10 emu/g (Chandradass et al., 2012; Kaur and Kaur, 2014). This small degree of magnetization can be due to the fact that a pure crystalline phase of magnesium ferrite nanoparticles is difficult to obtain by coprecipitation method. Gel combustion methods have been reported as better synthesis routes to achieve particles with improved superparamagnetic properties and a saturation magnetization value of 22.7 emu/g (Chandradass et al., 2012), yet smaller than that of the bulk magnesium ferrite (33.4 emu/g) (Maensiri et al., 2009).

Calcium ferrite nanoparticles crystallize in a normal spinel structure, in which the tetrahedral and octahedral sites are occupied by Ca^{2+} and Fe^{3+} ions, respectively. The sol−gel method is one of the most used for the synthesis of calcium ferrite nanoparticles, providing a low-cost production of magnetic materials with good homogeneity and high purity (Sulaiman et al., 2015; Saldívar-Ramírez et al., 2014; Khanna and Verma, 2013a,b). Using polyvinylalcohol as surfactant, calcium ferrite nanoparticles with orthorhombic structure, good purity, and average crystal size of 16.8 nm, were obtained by sol−gel method (Sulaiman et al., 2016). These particles exhibited good superparamagnetic behavior, with a high saturation magnetization of 59.3 emu/g. However, the same research team has shown that calcium ferrite nanoparticles with improved superparamagnetic properties and an even higher saturation magnetization, 88.3 emu/g, can be obtained

by a sol−gel route and without surfactant, which was found to be responsible for some surface defects that cause a lower magnetization (Sulaiman et al., 2015).

The knowledge on the synthesis of magnesium and calcium mixed ferrites is still very poor. Nevertheless, some studies point to promising features for these kinds of particles. It has been reported that a higher concentration of Ca^{2+} leads to a more appropriate superparamagnetic behavior, with increasing saturation magnetization and a coercivity decrease (Saldívar-Ramírez et al., 2014). Moreover, the hysteresis loss for $Mg_{0.5}Ca_{0.5}Fe_2O_4$ was found to be higher than that of magnesium ferrite nanoparticles (Hirazawa et al., 2008).

11.2.4 CORE−SHELL NANOPARTICLES

In the biomedical research field, core−shell nanoparticles have been the focus of attention over the past two decades, because of several advantages over simple nanoparticles (Chatterjee et al., 2014). This type of nanoparticles consists of a core made of a material, coated with another material. The major benefits associated with this type of structure rely on properties improvement, also avoiding undesirable effects of the nanoparticles. For biomedical applications, the use of core−shell structures offers huge advantages, such as less cytotoxicity, higher biocompatibility, better conjugation with other bioactive molecules, and increased thermal and chemical stability (Chatterjee et al., 2014; Law et al., 2008; Sounderya and Zhang, 2008).

Poly(ethylene glycol) (PEG) is one of the most used materials for the shell of nanostructures and PEGylation (coating with PEG) is a favored way to ensure biocompatibility. PEG prevents the adsorption of blood proteins, primarily due to steric repulsion, increasing the retention time of nanomagnets in the circulation system (Illés et al., 2014). Two main methods of PEGylation have been developed. The first consists on the physicochemical binding of PEG (or functionalized PEG) to the bare or previously modified surface of magnetic nanoparticles. The other consists on chemical coupling, either in situ during the particle precipitation, or by chemisorption of functionalized PEG on the nanoparticle surface (Illés et al., 2014; Veiseh et al., 2010; Mishra et al., 2010; Thong-On et al., 2012).

Silica is also a widely spread shell material, being a particularly beneficial coating for nanoparticles since it can be easily functionalized and is resistant to degradation within a cellular environment, whilst still being biocompatible. Previous studies have shown that internalized silica-coated magnetic nanoparticles are biocompatible with stem cells (Huang et al., 2008; Kim et al., 2011). Nickel/silica core−shell nanoparticles were obtained using the coprecipitation method for the nickel core, the silica shell growth being attained by tetraethyl orthosilicate (TEOS) hydrolysis with microheterogeneous templating (Rodrigues et al., 2014). Distinct protocols provided different shell thicknesses. In AOT/cyclohexane/water (AOT: bis(2-ethylhexyl)sulfosuccinate) reverse micelles, shell growth is limited by the size of water pools (Table 11.1), while TEOS hydrolysis in

Table 11.1 Hydrodynamic Diameter (Obtained by Dynamic Light Scattering) of Nickel Nanoparticles With and Without a Silica Shell, Prepared by Several Synthesis Methods

		Hydrodynamic Diameter (nm)		
			Number Distribution	
Synthesis Method	[TEOS]:[Ni]	Intensity Distribution	Core	Shell Thickness
Aqueous CTAB solution; TEOS added in AOT/cyclohexane	0:1	88 ± 7	84 ± 7	–
	10:1	157 ± 16	84 ± 7	34 ± 7
	30:1	175 ± 24	84 ± 7	42 ± 12
	60:1	185 ± 21	84 ± 7	48 ± 10
Covered with one AOT layer	0:1	100 ± 9	95 ± 13	–
Covered with one DOPG layer	0:1	79 ± 6	76 ± 6	–

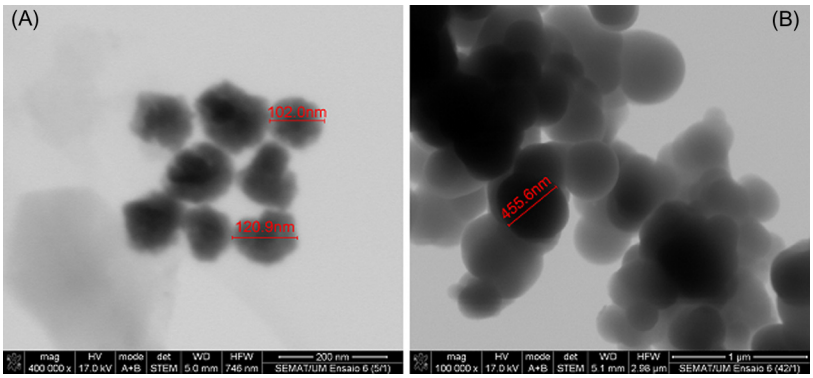

FIGURE 11.7

SEM images of nickel nanoparticles coated with silica shell. (A) [TEOS]/[Ni] = 5:1 (TEOS added in AOT/cyclohexane solution); (B) [TEOS]/[Ni] = 42:1 (TEOS added in ethanol solution with MDA).

Reprinted from Rodrigues, A.R.O., Gomes, I.T., Almeida, B.G., Araújo, J.P., Castanheira, E.M.S., Coutinho, P. J.G., 2014. Magnetoliposomes based on nickel/silica core/shell nanoparticles: synthesis and characterization. Mater. Chem. Phys. 148, 978–987 with permission from Elsevier.

ethanol using mercaptododecanoic acid (MDA) as binding agent provided larger shells (Fig. 11.7). The coverage of nickel nanoparticles with a surfactant (AOT) or phospholipid (DOPG) layer was also attempted (Table 11.1) (Rodrigues et al., 2014).

11.3 MAGNETOLIPOSOMES: SYNTHESIS AND CHARACTERIZATION

As already mentioned, magnetoliposomes are promising multifunctional nanosystems that combine liposomes with magnetic nanoparticles and can be used in a great array of biomedical applications. Over the past decade, significant importance has been invested in the development of these hybrid nanosystems and numerous variations of magnetoliposomes have been proposed (Monnier et al., 2014). There are different approaches to associate magnetic nanoparticles with liposomes, resulting in distinct structures of magnetoliposomes. The magnetic nanoparticles can be encapsulated directly into the aqueous lumen of the liposomes (Rodrigues et al., 2014), embedded in between the lipid bilayer (Bonnaud et al., 2014; Amstad et al., 2011), and a more recent approach describes the conjugation of iron oxide nanoparticles to the liposome surface (Floris et al., 2011). Moreover, concerning the particles encapsulation into the lumen of liposomes, the magnetic nanoparticles can be dispersed in the inner aqueous phase forming aqueous magnetoliposomes (AMLs), or the inner aqueous phase can be replaced by a magnetic nanoparticles cluster creating solid magnetoliposomes (SMLs) (Fig. 11.8) (Rodrigues et al., 2015, 2016).

Different applications require distinct structures for magnetoliposomes, and the spatial location of the magnetic nanoparticles within the liposomes is an important factor. For example, in drug delivery applications, the location of the nanoparticles within the lipid bilayer could be advantageous, as the nanoparticles may interfere with coencapsulated compounds before fusion with the cells of interest. Conversely, for imaging, the encapsulation of magnetic nanoparticles in the inner lumen of liposomes is preferred and has been the most studied magnetoliposomal structure (Monnier et al., 2014). The AMLs have a more advantageous structure for the loading of compounds, as they can carry both hydrophilic and

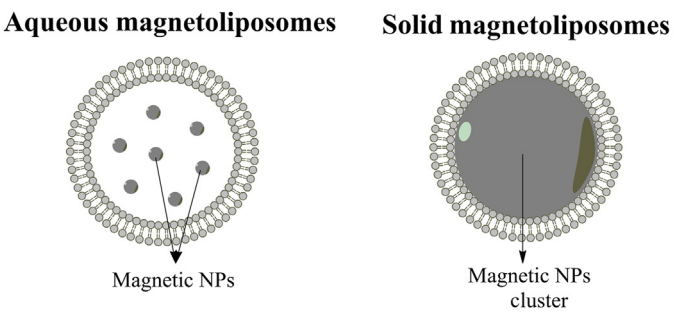

FIGURE 11.8

Schematic representation of aqueous magnetoliposomes (AMLs) and solid magnetoliposomes (SMLs).

hydrophobic/lipophilic drugs, while SMLs can only carry hydrophobic ones. However, SMLs have shown better magnetic properties, because SMLs keep almost the same magnetic properties as the neat nanoparticles (Zhang et al., 2012), while AMLs display poor magnetic characteristics, similar to those of the aqueous ferrofluid (García-Jimeno et al., 2011).

Magnetoliposome stability is also important and can be manipulated by lipid bilayer composition. The chemical stability of the system is related to liposome composition, while physical stability is associated with the aggregation and fusion of the vesicles. Working on the lipid bilayer formulation, with the insertion of specific molecules, an ideal nanosystem can be designed. Additionally, the inclusion of electrical charges into the liposome surface will improve the physical stability of the magnetoliposomes, as the electrostatic repulsion reduces vesicle fusion and aggregation. The addition of cholesterol will prevent compound release, as it will decrease membrane permeability and improve the chemical stability. Egg-yolk phosphatidylcholine (egg-PC) liposomes with cholesterol (70:30) are commonly used as models of cell membranes (Toniolo et al., 1996).

Concerning the application of magnetoliposomes in cancer therapy, in order to specifically target cancer cells, it is possible to attach antibodies (Elmi and Sarbolouki, 2001), use PEG-folate conjugates to target folate receptors (overexpressed in cancer cells) (Pradhan et al., 2010), and incorporate small peptides that target specific membrane proteins (Jain et al., 2003). Recently, it was shown that the use of magnetoliposomes tagged with folate resulted in superior cell uptake of the well known anticancer drug doxorubicin (Bothun et al., 2011). The inclusion of the anionic lipid cholesteryl hemisuccinate in magnetoliposomes is also promising, as it allows them to be pH-sensitive, which is a relevant feature considering that tumor cells have lower pH than normal cells. These liposomes fuse after the pH is lowered below a critical value between 4.0 and 6.7 (Hafez et al., 2000).

No less important are the structural and the magnetic properties of magnetoliposomes. To be suitable for biomedical applications, the nanosystems must have sizes around or below 100 nm and should present superparamagnetic properties at room temperature. Different methods have been proposed for the synthesis of magnetoliposomes, and depending on the preparation method, different structures and physicochemical or magnetic characteristics are obtained. The structural and magnetic characterization of these systems is challenging, due to all components and all the contributions that they have. The sizes of these nanosystems have been measured mostly by dynamic light scattering (DLS) and electronic microscopy (TEM or SEM); the magnetic properties have been studied by the hysteresis cycle at room temperature (Rodrigues et al., 2016).

11.3.1 AQUEOUS MAGNETOLIPOSOMES

One of the simplest protocols used to obtain AMLs is the so-called ethanolic injection method. This is a simple technique, which provides a reasonably

homogeneous population, although rather dilute. The advantages of ethanolic injection include its potential for scale-up, the simplicity of the procedure, low cost, and low expenditure of time. Small liposomes in a size range of 30−110 nm are generally obtained. This method consists of the injection of a lipid solution in ethanol, under vigorous vortexing, to an aqueous solution of nanoparticles, above the melting transition temperature of the lipids. After encapsulation, the ferrofluid is washed with water and purified by magnetic decantation and centrifugation, to remove all the nonencapsulated nanoparticles (Rodrigues et al., 2014).

Some recent results have shown that the presence of small magnetic nanoparticles of nickel ferrite or manganese ferrite have a negligible influence on the size of AMLs. Liposomes of egg lecithin containing nickel ferrite nanoparticles exhibit diameters of 92 ± 18 nm (Rodrigues et al., 2015), while those entrapping manganese ferrite nanoparticles present a size distribution of 82 ± 13 nm (Rodrigues et al., 2016), compared with 92 ± 10 nm for the neat egg-PC liposomes (all values obtained by DLS measurements). However, the same was not observed for magnetoliposomes based on nickel/silica core/shell nanoparticles, where the presence of larger nanoparticles contributes to an increase of liposomes diameter. Nevertheless, the encapsulation of these particles into liposomes of egg-PC (forming AMLs) prevents nanoparticle aggregation, improving their stability (Table 11.2) (Rodrigues et al., 2014).

Other techniques for the synthesis of AMLs have been described. Egg-PC AMLs containing lauric acid−coated manganese ferrite nanoparticles were previously prepared by Pradhan and coworkers, using two different methods: thin film hydration and double emulsion, resulting in magnetoliposomes of *ca.* 300 nm diameter (Pradhan et al., 2007). This size is significantly larger than those

Table 11.2 Hydrodynamic Diameter (Obtained by DLS) of Nickel Nanoparticles With and Without Silica Shell and of Aqueous Magnetoliposomes Containing the Same Nickel Nanoparticles (With and Without Silica Shell)

System	[TEOS:Ni]	Hydrodynamic Diameter (nm)
Nickel nanoparticles (obtained in aqueous CTAB solution, TEOS added in AOT/cyclohexane)	0:1	88 ± 7
	10:1	157 ± 16
	20:1	175 ± 24
Egg-PC magnetoliposomes with nickel nanoparticles	0:1	103 ± 20
	10:1	126 ± 33
	20:1	135 ± 34

obtained using the ethanolic injection method (Rodrigues et al., 2016). Pradhan et al. also reported that PEGylated egg-PC:cholesterol 2:1 AMLs prepared by thin film hydration (with diameters ~188 nm) are the most promising systems (amongst a series of different egg-PC:chol compositions) for hyperthermia treatment of cancer (Pradhan et al., 2007). The reverse-phase method, followed by sequential extrusion, has also been employed for the preparation of this type of magnetoliposomes, addressing the treatment of inflammation (García-Jimeno et al., 2011).

Regarding the magnetic properties of AMLs, it has been shown that they generally present poor magnetic properties (García-Jimeno et al., 2011). AMLs based on manganese ferrite nanoparticles have shown to be superparamagnetic at room temperature. In terms of hysteresis, AMLs presented similar behavior to the neat nanoparticles, with small coercive field values of 6.30 and 8.43 Oe, for $MnFe_2O_4$ nanoparticles and AMLs, respectively (Rodrigues et al., 2017). Furthermore, $MnFe_2O_4$ nanoparticles are superparamagnetic, but not the other components of magnetoliposomes, as both water and lipids are diamagnetic, leading to a strong decrease of the maximum saturation magnetization of the combined nanosystem.

Recent investigations on the fusion capability of AMLs with models of cell membranes indicated a promising use of magnetoliposomes as nanocarriers for both hydrophilic (in the inner aqueous volume) and hydrophobic (in the lipid bilayer) drugs, as they can be guided with an external magnetic field and can release the encapsulated drugs by fusion with membranes. Membrane fusion with giant unilamellar vesicles (GUVs) (used as models of cell membranes) was confirmed by Förster resonance energy transfer (FRET) assays, for AMLs containing nickel/silica core−shell nanoparticles (Rodrigues et al., 2014), nickel ferrite nanoparticles (Rodrigues et al., 2015), and manganese ferrite nanoparticles (Rodrigues et al., 2016). In this kind of experiment, a pair of donor-acceptor molecules is included in the magnetoliposome moiety and fluorescence emission of the system is measured, exciting only the energy donor, before and after the interaction with model membranes. The nitrobenzoxadiazole (NBD)-labeled lipid NBD-C_6-HPC (or NBD-C_{12}-HPC) was used as the energy donor (through the fluorophore, NBD) and the hydrophobic dye Nile Red (a widely used lipid probe), as the energy acceptor. This donor-acceptor pair (NBD/Nile Red) has a significant spectral overlap (Fig. 11.9, inset), so the energy transfer between these two molecules is expected to be efficient, if their distance is below 100 Å. A decrease in energy transfer from NBD to Nile Red is observed upon magnetoliposome interaction with GUVs (Fig. 11.9).

As FRET efficiency strongly depends on the distance between donor and acceptor molecules, the FRET decrease confirms membrane fusion between magnetoliposomes and models of cell membranes, with the formation of a larger membrane and consequential increase in the donor−acceptor distance (Fig. 11.10).

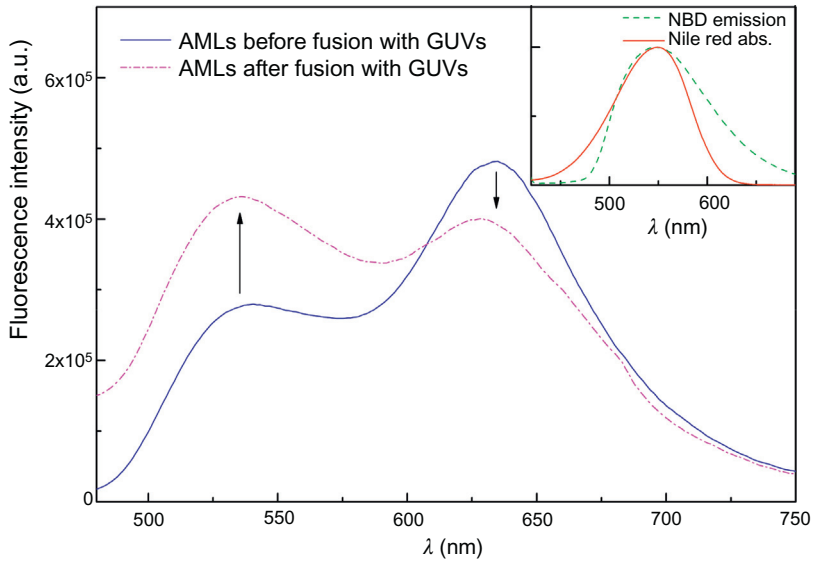

FIGURE 11.9

Fluorescence spectra of AMLs of egg-PC and Ni/silica core–shell nanoparticles containing both NBD-C_6-HPC (1×10^{-6} M) and Nile Red (2×10^{-6} M), before and after interaction with GUVs. Inset: spectral overlap (spectra are normalized) between the fluorescence emission of the donor (NBD-C_6-HPC) and the absorption of the acceptor (Nile Red).

Reprinted from Rodrigues, A.R.O., Gomes, I.T., Almeida, B.G., Araújo, J.P., Castanheira, E.M.S., Coutinho, P.J.G., 2014. Magnetoliposomes based on nickel/silica core/shell nanoparticles: synthesis and characterization. Mater. Chem. Phys. 148, 978–987 with permission from Elsevier.

11.3.2 SOLID MAGNETOLIPOSOMES

SMLs may be more promising for some biomedical applications, as they present a better magnetic response when compared with AMLs. Typically, the synthesis of SMLs consisted on the growth of a second lipid layer around magnetic nanoparticles covered by a monolayer (previously synthesized in the presence of lipids) (Lubbe et al., 1999; Meledandri et al., 2011). SMLs can also be obtained by mixing small liposomes (obtained by strong sonication with a tip) with magnetic nanoparticles, followed by dialysis (Andresen et al., 2005). The method described by Meledandri and coworkers (Meledandri et al., 2011) was followed to prepare SMLs of the anionic phospholipid DOPG containing nickel nanoparticles (Rodrigues et al., 2014) and exhibiting sizes below 100 nm (Fig. 11.11).

More recently, a new method for the synthesis of SMLs with improved magnetic properties was described, involving a balance between hydrophilic and

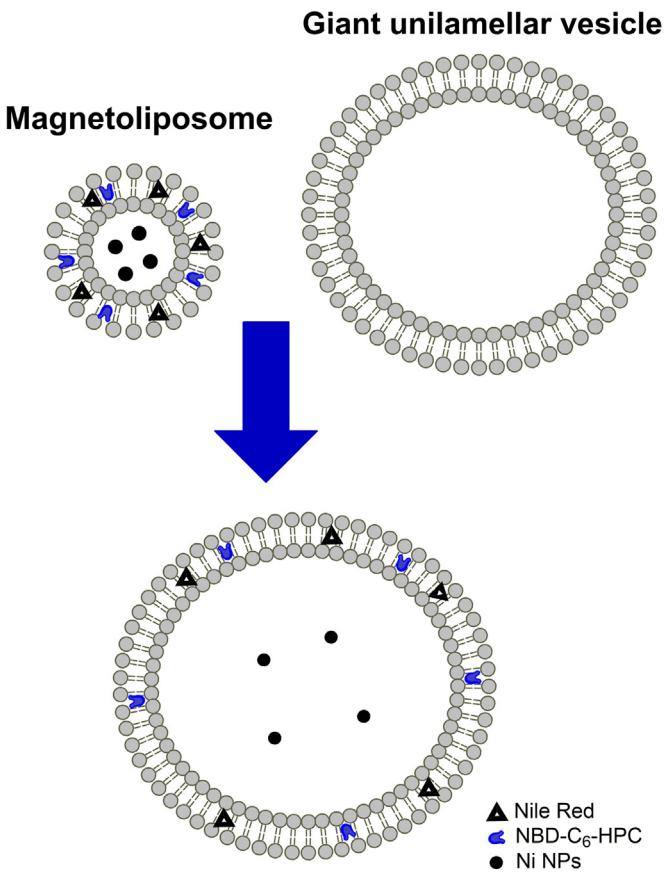

FIGURE 11.10

Schematic illustration of the fusion between GUVs and magnetoliposomes labeled with both NBD-C_6-HPC and Nile Red.

Reprinted from Rodrigues, A.R.O., Gomes, I.T., Almeida, B.G., Araújo, J.P., Castanheira, E.M.S., Coutinho, P.J.G., 2014. Magnetoliposomes based on nickel/silica core/shell nanoparticles: synthesis and characterization. Mater. Chem. Phys. 148, 978–987 with permission from Elsevier.

hydrophobic forces (Rodrigues et al., 2015). Concerning the fact that most of the magnetic nanoparticles with great magnetic properties require a calcination step, this new method stands out because the coating of nanoparticle cluster with the lipid bilayer occurs only after the nanoparticle synthesis, with no risk of "burning" the lipid bilayer. The effective formation of a lipid bilayer surrounding the magnetic nanoparticles cluster by this new method was proved by FRET assays

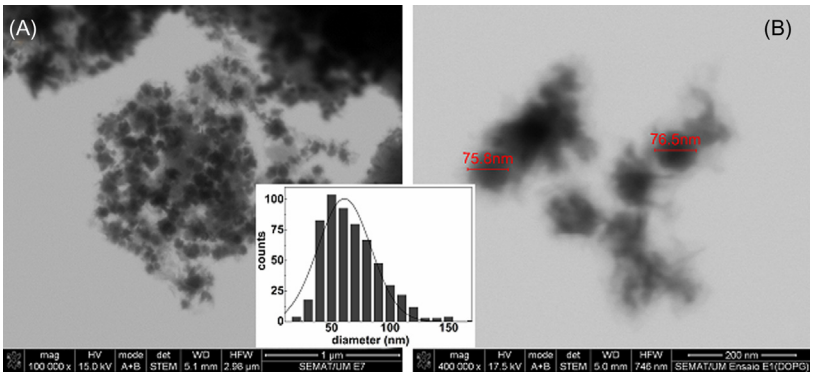

FIGURE 11.11

(A), (B) SEM images of solid magnetoliposomes of nickel nanoparticles covered by a DOPG lipid bilayer with different magnifications. Inset: Particles size histogram of image A and fitting to a Gaussian distribution.

Reprinted from Rodrigues, A.R.O., Gomes, I.T., Almeida, B.G., Araújo, J.P., Castanheira, E.M.S., Coutinho, P. J.G., 2014. Magnetoliposomes based on nickel/silica core/shell nanoparticles: synthesis and characterization. Mater. Chem. Phys. 148, 978–987 with permission from Elsevier.

Table 11.3 Magnetic Data Obtained From the Loops

	H_c (Oe)	M_s (emu/g)	M_r (emu/g)	M_r/M_s
$MnFe_2O_4$ nanoparticles	6.30	36.00	0.58	0.02
SMLs based on $MnFe_2O_4$ nanoparticles	4.22	34.16	0.90	0.03
AMLs based on $MnFe_2O_4$ nanoparticles	8.43	1.17	0.08	0.07

Coercivity field (H_c), saturation magnetization (M_s), remnant magnetization (M_r), and magnetic squareness ratio (M_r/M_s) of neat $MnFe_2O_4$ nanoparticles, SMLs based on $MnFe_2O_4$ nanoparticles and AMLs based on $MnFe_2O_4$ nanoparticles.

(Rodrigues et al., 2015). DLS measurements of DOPG SMLs, containing either nickel ferrite nanoparticles or manganese ferrite nanoparticles, indicated that this method yields SMLs with larger diameters than the previous methods, yet smaller or around 150 nm, and therefore suitable for biomedical applications (Rodrigues et al., 2015, 2016).

Although both AMLs and SMLs exhibit superparamagnetic properties with low coercivity and remnant magnetization, and magnetic squareness values below 0.1 (Table 11.3), SMLs are preferable in terms of magnetic properties, as observed from the hysteresis cycles of both types of magnetoliposomes and neat nanoparticles (Fig. 11.12). A similar behavior was observed for

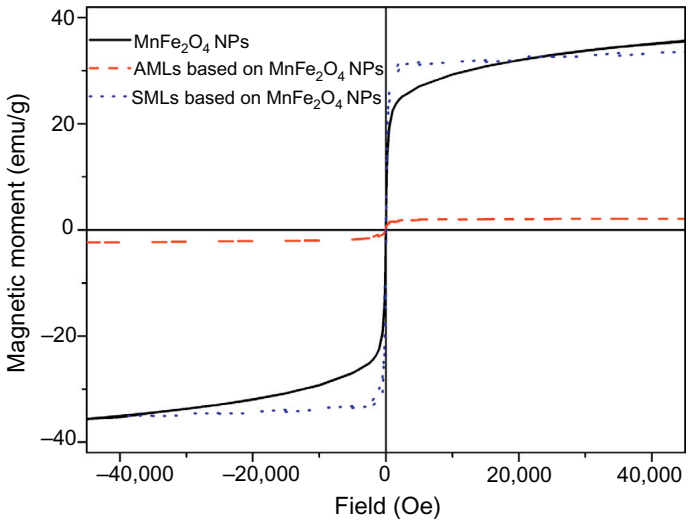

FIGURE 11.12

Magnetization hysteresis cycles of neat $MnFe_2O_4$ nanoparticles of SMLs based on $MnFe_2O_4$ nanoparticles and AMLs based on $MnFe_2O_4$ nanoparticles.

magnetoliposomes based on magnetite nanoparticles (Zhang et al., 2012; García-Jimeno et al., 2011). SMLs based on manganese ferrite nanoparticles have a saturation magnetization near to that of neat $MnFe_2O_4$ nanoparticles, due to the structure of the magnetic nanoparticle cluster. Here, the clearer saturation of the hysteresis loop (Fig. 11.12, blue line) shows that interparticle magnetic interaction favors the magnetic moment alignment, due to the degree of clustering inside the lipid bilayer.

Pointing to future applications of both AMLs and SMLs based on manganese ferrite nanoparticles in cancer therapy, a new potent antitumor compound, a thienopyridine derivative (Queiroz et al., 2010), was incorporated into both types of magnetoliposomes. This potential antitumor drug is promising, due to its inhibitory activity on the growth of several human tumor cell lines (melanoma, breast adenocarcinoma, and nonsmall cell lung cancer), and it has also shown a very low affinity for the multidrug resistance protein MDR1, which promotes drug resistance in cells (Costa et al., 2014). The drug-loaded magnetoliposomes confirmed that this potential antitumor drug can be carried in both AMLs and SMLs, mainly in the lipid bilayer, due to its hydrophobic nature. Moreover, the compound-loaded magnetoliposomes, either solid or aqueous, also interact with cell membrane models (GUVs) by fusion (Rodrigues et al., 2016), as was previously proven for the unloaded systems (Rodrigues et al., 2015).

11.4 APPLICATIONS IN CANCER THERAPY

As was demonstrated in previous sections, the scientific community has been making a great effort to develop and improve magnetoliposomes, ranging from general biophysical studies to triggered release demonstrations, in order to invert the dramatic cancer statistics on the future (Monnier et al., 2014). This versatile nanosystem is promising, not only in cancer therapy but also in diagnosis, as it can provide combined synergistic drug delivery, hyperthermia treatment at specific target sites and coinstantaneous MRI, in a single bionanosystem. This new approach to cancer therapy aims to replace the currently traditional high spectrum chemotherapy, which leads to severe problems in patients, such as the high drug dosage needed, low efficacy, and significant side effects.

11.4.1 MAGNETIC HYPERTHERMIA

Magnetic hyperthermia therapy consists of targeting magnetic nanoparticles to tumor tissues, followed by the application of an alternating current (AC) magnetic field that induces heat. In hyperthermia, hysteresis losses and Néel relaxation loss are the most important mechanisms of energy loss. Superparamagnetic particles have no hysteresis, generating heat by relaxation losses, mainly by Néel relaxation. When placed under an AC magnetic field, the moments of superparamagnetic nanoparticles randomly flip the magnetization direction between the parallel and antiparallel spin orientation. This random orientation converts dissipated magnetic energy, due to losses during magnetization relaxation, into thermal energy. Energy loss occurs either through physical rotation of the nanoparticles in fluid, Brownian relaxation, or by rotation of the atomic magnetic moment within the particles themselves, Néel relaxation. Considering that tumor cells are more heat-sensitive than normal tissues, magnetic nanoparticles can be used to deliver a toxic amount of thermal energy to tumor tissues and cause necrosis of cancer cells by hyperthermia. The greatest advantage associated with thermotherapy is that it allows the heating to be restricted to the tumor area so healthy cells are preserved. The specific absorption rate (SAR) is the key parameter that determines heating generation in the tissue and describes the energy amount converted into heat per time and mass. The SAR is proportional to the rate of temperature increase, for the adiabatic case, and is expressed in Watt per kilogram (Eq. (11.3)),

$$\mathrm{SAR} = 4.1868\frac{P}{m_e} = C_e\frac{dT}{dt} \tag{11.3}$$

where P is the electromagnetic wave power absorbed by the sample, m_e is the mass of the sample, and C_e is the specific heat capacity of the sample.

The tissue electrical permeability and conductivity cause a SAR variation and local high temperatures, known as hot spots. In order to achieve better control of

the energy irradiation, low-frequency magnetic waves ~100 kHz are used in hyperthermia. The magnetic relaxation of the magnetic moments plays an important role in the SAR of ferrofluids and can be determined theoretically by Eq. (11.4) (Laurent et al., 2011),

$$\mathrm{SAR} = 4.1868\pi\mu_0^2 \frac{\varphi M_s^2 V}{10,000kT} H_0^2 \nu \frac{2\pi\nu\tau}{1+(2\pi\nu\tau)^2} \tag{11.4}$$

where V is the volume of superparamagnetic material, K the anisotropy constant, T the temperature, φ the volume fraction of magnetic material, M_s the saturation magnetization, ν the frequency of the alternate current magnetic field, H_0 is the magnetic field intensity, and τ is the relaxation time.

If the AC magnetic field interacts with intracellular ions, Eddy currents can be formed, leading to significant heating in normal tissues. In this way, normal cells can be damaged, so a limitation must be imposed. As SAR is directly proportional to the frequency and magnitude of the applied field, and in order to avoid any damaging of healthy tissues, $H_0\nu$ factor should not exceed an experimental value estimated as 5×10^9 A $m^{-1}s^{-1}$ (Hergt and Dutz, 2007; Shubitidze et al., 2015).

Gordon and collaborators were the first to address temperature treatment for cancer therapy (Gordon et al., 1979); since then, many research groups have been focused in the development of hyperthermia agents. The use of magnetic materials as hyperthermia agents date back to 1957, when Gilchrist and his group heated various tissue samples with maghemite nanoparticles exposed to a 1.2 MHz magnetic field (Gilchrist et al., 1957). Since then, several researchers have reported encouraging results using magnetic nanoparticles as hyperthermia agents and numerous publications have been published describing a variety of different types of magnetic materials.

The use of magnetoliposomes for hyperthermia therapy improves colloidal stability of the magnetic nanoparticles, prevents agglomeration in vivo, and guarantees biocompatibility. The inclusion of ligands for specifically target cancer cells, as in drug delivery, also can provide a better local heating for the thermal treatment (Escalona et al., 2016). Cancer cell membrane contains more anionic lipids than normal cells, leading to an overall negatively charged cell surface (Chen et al., 2016). Regarding this, the use of cationic magnetoliposomes have shown to be a promising approach, as the accumulation of magnetic nanoparticles in tumor cells can be enhanced due to electrostatic interactions. Kobayashi has demonstrated the efficacy of intracellular hyperthermia, using cationic liposomes in animals with several types of tumors (Kobayashi, 2011). In this experiment, cationic magnetoliposomes containing a magnetite amount of 3 mg/tumor were used. The magnetoliposomes were directly injected into solid tumors and the animals were irradiated several times for 30 min, with an alternating magnetic field of 118 kHz. The results showed an evident decrease in the volume of tumors, and a tumor regression in 96% of the animals (Kobayashi, 2011).

Furthermore, antitumor immunity has already been observed in hyperthermia treatment. Experiments in T-9 rat glioma model, in which T-9 cells were transplanted into each femur of rats and where only one of the tumors was subjected to hyperthermia, an effective regression of tumor volume was detected in the incident tumor and in the tumor without radiation incidence (Yanase et al., 1998). Here, an immunohistochemical assay demonstrated that natural killer cells and $CD8^+$ and $CD4^+$ T-cells migrated into the heated tumor and also into the tumor without thermal treatment. Therefore, magnetic hyperthermia is indeed a promising tool for cancer treatment. It can make use of local heating to kill cancer cells and also induce biological responses, being able to kill tumors located far from hyperthermia incidence and metastatic cancer cells.

11.4.2 MAGNETOLIPOSOMES AS ANTICANCER DRUG NANOCARRIERS

Most of the anticancer drugs used in chemotherapy are severely toxic and cause systemic side effects. Magnetoliposomes are an alternative approach to conventional chemotherapy that compromises improved treatment and overcomes systemic toxicity problems. Drug delivery based on magnetoliposomes stands out compared to other nanosystems, as it allows the concentration of the nanocarriers, loaded with potent anticancer drugs, in the treatment area of patient organs by magnetic forces, often augmented by magnetic agglomeration. Furthermore, the ability to magnetically guide transported drugs and focus them to specific sites in the human body allows a lower drug dosage and a more efficient therapy.

The flow of magnetoliposomes in blood results from the competition between magnetic forces of the magnetic nanoparticles in blood circulation and magnetic forces applied by the external magnetic field. The magnetic fluid is localized in the site of interest when the magnetic forces are exerted on linear blood flow of the arteries or capillaries (Meledandri et al., 2011). The magnetic force of attraction that can be exerted on magnetoliposomes by the external field is proportional to the saturation magnetization of encapsulated superparamagnetic nanoparticles, and is given by Eq. (11.5),

$$\overrightarrow{F_m} = V(\overrightarrow{M_s} \cdot \nabla)\ \overrightarrow{B} \tag{11.5}$$

where F_m is the magnetic force experienced by the particle, V the particle volume, and B the magnetic field intensity.

In order to achieve an appropriate local release and avoid premature drug liberation in the plasma or interstitial space, magnetoliposomes are targeted to cancer cells through surface functionalization. Drug release can be induced by physicochemical variations of the microenvironment, such as temperature or pH, depending on the functionalization of magnetoliposomes. Therefore, besides physical and magnetic properties, the surface functionalization is also important and

compromises the efficacy of the magnetically guided drug targeting. The external magnetic field geometry, strength and duration, and the injection route also influence the treatment. They are determined by physiological parameters of the patient, such as body weight, blood volume, cardiac output, peripheral resistance of the circulatory system, and organ function (Allen et al., 1997). Magnetic-guided transport of anticancer drugs requires equipment able to generate high-gradient external magnetic fields, to allow the guidance and concentration of the drugs after injection, into the target tissues. Such high fields are generated by rare-earth permanent magnets, usually neodymium-iron-boron magnets (Estelrich et al., 2015).

Investigations on the triggered release of anticancer drugs using magnetoliposomes have shown increased concentration of the drugs on the specific site of interest after magnetic targeting. Zhang et al. investigated the pharmacokinetics, in vivo distribution, and cytotoxicity of paclitaxel (a FDA-approved cancer chemotherapeutic agent) in a comparative study between liposomes and magnetoliposomes (Zhang et al., 2005). The results of this study evidenced a superior antitumor efficiency for the formulation of paclitaxel loaded in magnetoliposomes, with drug distribution localized higher in tumor tissues than in plasma, heart, liver, spleen, lung, and kidney tissues. Moreover, in the presence of an external magnetic field, magnetoliposomes reached concentration peak very quickly, attaining 19.85 μg of drug per g of mice weight at ¼ h (Zhang et al., 2005).

Brain tumor treatment has been one of the most challenging among all, due to the blood-brain barrier (BBB). This is a highly selective semipermeable membrane that obstructs the influx of most compounds from blood to brain, thus blocking the delivery of therapeutic agents to brain. Magnetoliposomes have shown to be a promising therapeutic approach for this kind of tumor. Ding and collaborators evaluated BBB transmigrability of magnetoliposomes in vitro, using a BBB model composed of human brain−sourced primary cells (Ding et al., 2014). Transferrin receptor, a BBB-specific transporter that allows transferrin to attach and cross BBB membrane (Hu et al., 2009), was embedded in the liposome surface and transmigration was evaluated for nanocarriers only with transferrin receptor, only with magnetic force (for guided delivery), and for the synergy of both. The results evidenced that, by means of magnetic force and transferrin receptor-mediated transportation, 50%−100% higher transmigration was obtained (Ding et al., 2014).

Moreover, investigations in vivo have already shown encouraging results for the use of magnetoliposomes in drug delivery. Cationic magnetic liposomes loaded with paclitaxel have shown 5−15 fold higher concentration in rats brain when magnetic controlled drug delivery was used (Zhao et al., 2012). The main problem within these amazing results, from the physical point of view, is that the magnetic field force decays rapidly with distance, limiting applications to relatively shallow targets in the human body. Despite the great results on small

animals, the problem of magnetic targeting in current investigation is to manipulate magnetic particles to deeper tissues, such as for humans, where the sites of interest are farther away from the magnet source. Although the use of common neodymium-iron-boron magnets achieves a 10−15 cm depth (Goodwin et al., 1999), this is not enough and recent studies have been proposing different approaches to a deeper penetration of the field in tissues (Mathieu and Martel, 2010). Magnetic resonance navigation that steers and tracks magnetic carriers in real time can be achieved with a clinical MRI scanner, upgraded with an insert of steering coils (Pouponneau et al., 2010). The high magnetic field (1.5 T) of the equipment enables the magnetic material to be fully magnetized throughout the body, even in deep tissues.

11.4.3 SYNERGISTIC THERMO/CHEMOTHERAPY

Magnetoliposomes appear to be a versatile nanodelivery system with high potential for combined therapy of cancer. The combination of both chemotherapy and magnetic hyperthermia functions in the same nanosystem can make use of the good capacities of individual therapies, controlled drug delivery, and thermal treatment, as well raise synergistic effects in cancer therapy. The presence of magnetic nanoparticles offers the possibility to guide the nanosystem to the site of interest by means of an external magnetic field. Moreover, the heat generated by local hyperthermia on the magnetic nanoparticles (after the application of an AC field) will trigger the fast release of encapsulated anticancer drugs and improve therapy efficiency, due to simultaneous application of hyperthermia and chemotherapy.

There are several mechanisms of action involved in the enhancement of chemotherapy by the application of hyperthermia, such as drug accumulation increase in the sites of interest and enhanced drug cytotoxicity at mild hyperthermia temperatures (Rao et al., 2010). Drug accumulation results from the hyperthermia effect on the physiological vasculature of the tumor, such as increased blood flow, perforation, and blood vessel pore size, which facilitates drug penetration in tumor tissues. Conversely, although drug cytotoxicity enhancement is not yet clear, several studies suggest that it can be related to cell membrane permeability, inhibition of DNA-repair, and acceleration of the cytotoxic chemical reactions at high temperatures (Issels, 2008).

The external magnetic field required for drug delivery alone requires high frequencies and amplitudes in order to control magnetic nanoparticle position. However, this strong field could lead to safety problems, as it could generate Eddy currents leading to nonspecific heating damaging of both healthy and cancer tissues. Regarding combined therapy, recent studies have shown that thermal enhancement of drug cytotoxicity occurs at mild hyperthermia temperatures and so combined therapy does not require temperatures as high as those for

hyperthermia alone (~43°C or higher) (Rao et al., 2010). Therefore, the SAR for combined therapy does not need to be especially high; lower frequencies and amplitudes of the external field could be used. Mild hyperthermia is easy, safe, and cost-effective, and can be performed at any medical facility.

Although the approach of combined therapy is relatively new, several research groups have already performed some promising studies with encouraging results. The permeability of magnetoliposomes based on cobalt ferrite nanoparticles was evaluated for combined treatment. Preliminary results suggested that the release of encapsulated carboxyfluorescein is strongly promoted by the application of a low-frequency alternating magnetic field (Nappini et al., 2010).

A little more forward study has shown that magnetoliposomes based on magnetite nanoparticles loaded with paclitaxel are promising for combined chemotherapy and hyperthermia. Here, in vitro cytotoxicity studies were performed in HeLa cell line, under an AC magnetic field of 10 kA/m intensity and 432 kHz frequency. When combined therapy was applied to magnetoliposomes with 100 nM paclitaxel, 89% of the cells were killed (Kulshrestha et al., 2012).

Itoh et al. also compared the efficacy of hyperthermia or chemotherapy alone, then combined, in a study where the enhancement of cisplatin and adriamycin cytotoxicity in human bladder cancer cell line was evaluated (Itoh et al., 2010). Alone, mild hyperthermia (~41°C) and chemotherapy, with a low drug concentration (20 μg/mL of cisplatin or 4 μg/mL of adriamycin) revealed unsuccessful treatment. However, when combined chemotherapy and hyperthermia were used, using the same temperature and drug concentration, the efficacy of treatment was significantly higher, with a 10-fold higher concentration obtained, when compared with chemotherapy alone. Moreover, it was also evidenced that drug dosage can also be reduced when chemotherapy is combined with mild hyperthermia, thus decreasing side effects of therapy (Itoh et al., 2010).

More recently, Hardiansyah and coworkers used AMLs containing citric acid–coated magnetite nanoparticles loaded with doxorubicin and found, again, that the integrated application of chemotherapy and magnetic hyperthermia (drug concentration of 1 μM and high-frequency magnetic field) is effective against colorectal cancer cells (Hardiansyah et al., 2014).

11.5 FUTURE PERSPECTIVES

In conclusion, magnetoliposomes are valuable nanosystems that combine the benefits of magnetic nanoparticles and liposomes. Due to their capabilities, many research groups have been dedicated to synthesis methods that improve these nanosystems and have also exhaustively studied their potentialities. The characterization of these hybrid nanostructures is one of the main drawbacks in the

development of these nanocarriers, as many complementary techniques are needed for full characterization. Considering the complexity of magnetoliposomes, a multidisciplinary expertise, from organic and inorganic chemistry to bio- and magnetic-physics and pharmacology are all required for a better understanding of these nanostructures.

Several obstacles to the synthesis, characterization, and biological applications of magnetoliposomes must be overcome, and ongoing investigation must not stop. Although liposomes are clinically established, studies published daily show that their efficacy can be enhanced. Different approaches on surface functionalization are being discovered regularly, and cell uptake can be further improved.

Magnetic nanoparticles also need to upgrade their properties, in order to provide a safer use of them, without "burning" healthy cells in thermal treatments. Regarding magnetic properties, magnetic nanoparticles with high SAR, together with the capability for magnetic-guided transport in the human body, are still to be found. The magnetic sources in clinical trials also need to be tailored for a treatment with greater penetration depth, still a problem for the in vivo application of magnetoliposomes.

Nevertheless, over the past decade, new concepts have been tested; progressive and promising work encourages the continuous study of magnetoliposome applications in dual cancer therapy. The scientific community believes that the intensive work in this field should continue; much more encouraging results are yet to come.

ACKNOWLEDGMENTS

Financial support by the Portuguese Foundation for Science and Technology (FCT) in the framework of the Strategic Funding UID/FIS/04650/2013 and UID/QUI/00686/2016 is acknowledged. A.R.O. Rodrigues thanks the FCT for SFRH/BD/90949/2012 PhD grant and funding to MAP-Fis Doctoral Program.

REFERENCES

Akbarzadeh, A., Samiei, M., Davaran, S., 2012. Magnetic nanoparticles: preparation, physical properties, and applications in biomedicine. Nanoscale Res. Lett. 7, 144–157.

Allen, L.M., Kent, T., Wolfe, C., Ficco, C., Johnson, J.M.T., 1997. A magnetically targetable drug carrier for paclitaxel. In: Häfeli, U., Schütt, W., Teller, J., Zbororowski, M. (Eds.), Scientific and Clinical Applications of Magnetic Carriers. Plenum Press, New York, pp. 481–494.

Altavilla, C., Ciliberto, E., 2011. Inorganic Nanoparticles: Synthesis, Applications, and Perspectives. CRC Press Taylor & Francis Group, New York.

Amstad, E., Kohlbrecher, J., Müller, E., Schweizer, T., Textor, M., Reimhult, E., 2011. Triggered release from liposomes through magnetic actuation of iron oxide nanoparticle containing membranes. Nano Lett. 11, 1664–1670.

Andresen, T.L., Jensen, S.S., Jorgensen, K., 2005. Advanced strategies in liposomal cancer therapy: problems and prospects of active and tumor specific drug release. Prog. Lipid Res. 44, 68–97.

Aono, H., Hirazawa, H., Naohara, T., Maeha, T., 2008. Surface study of fine $MgFe_2O_4$ ferrite powder prepared by chemical methods. Appl. Surf. Sci. 254, 2319–2324.

Babes, L., Denizot, B., Tanguy, G., Le Jeune, J.J., Jallet, P.J., 1999. Synthesis of iron oxide nanoparticles used as MRI contrast agents: a parametric study. Colloid Interface Sci. 212, 474–482.

Baek, M.J., Park, J.Y., Xu, W., Kattel, K., Kim, H.G., Lee, E.J., et al., 2010. Water-soluble MnO nanocolloid for a molecular T_1 MR imaging: a facile one-pot synthesis, in vivo T_1 MR images, and account for relaxivities. ACS Appl. Mater. Interfaces 2, 2949–2955.

Bamzai, K.K., Kour, G., Kaur, B., Arora, M., Pant, R.P., 2013. Infrared spectroscopic and electron paramagnetic resonance studies on Dy substituted magnesium ferrite. J. Magn. Magn. Mater. 345, 255–260.

Bao, Y., Pakhomov, A.B., Krishnan, K.M., 2006. Brownian magnetic relaxation of water-based cobalt nanoparticle ferrofluids. J. Appl. Phys. 99, 107–114.

Baumgartner, J., Bertinetti, L., Widdrat, M., Hirt, A.M., Faivre, D., 2013. Formation of magnetite nanoparticles at low temperature: from superparamagnetic to stable single domain particles. PLoS One 8, 57070–57076.

Bonnaud, C., Monnier, C.A., Demurtas, D., Jud, C., Vanhecke, D., Montet, X., 2014. Insertion of nanoparticle clusters into vesicle bilayers. ACS Nano 8, 3451–3460.

Bothun, G.D., Lelis, A., Chen, Y., Scully, K., Anderson, L.E., Stoner, M.A., 2011. Multicomponent folatetargeted magnetoliposomes: design, characterization, and cellular uptake. Nanomedicine: NBM 7, 797–805.

Bulte, J.J.W., Cuyper, M., Despres, D., Frank, J.A., 1999. Short vs. long-circulating magnetoliposomes as bone marrow-seeking MR contrast agents. J. Magn. Reson. Imaging 9, 329–335.

Cabrera, L.I., Somoza, A., Marco, J.F., Serna, C.J., Morales, M.P., 2012. Synthesis and surface modification of uniform MFe_2O_4 (M = Fe, Mn, and Co) nanoparticles with tunable sizes and functionalities. J. Nanopart. Res. 14, 1–14.

Carta, D., Casula, M.F., Floris, P., Falqui, A., Mountjoy, G., Boni, A., et al., 2010. Synthesis and microstructure of manganese ferrite colloidal nanocrystals. Phys. Chem. Chem. Phys. 12, 5074–5083.

Chandradass, J., Jadhav, A.H., Kim, K.H., Kim, H., 2012. Influence of processing methodology on the structural and magnetic behavior of $MgFe_2O_4$ nanopowders. J. Alloys Compd. 517, 164–169.

Chatterjee, K., Sarkar, S., Rao, K.J., Paria, S., 2014. Core/shell nanoparticles in biomedical applications. Adv. Colloid Interface Sci. 209, 8–39.

Chen, B., Le, W., Wang, Y., Li, Z., Wang, D., Ren, L., et al., 2016. Targeting negative surface charges of cancer cells by multifunctional nanoprobes. Theranostics 6, 1887–1898.

Costa, C.N.C., Hortelão, A.C.L., Ramos, J.M.F., Oliveira, A.D.S., Calhelha, R.C., Queiroz, M.-J.R.P., et al., 2014. A new antitumoral Heteroarylaminothieno[3,2-*b*] pyridine derivative: its incorporation into liposomes and interaction with proteins monitored by fluorescence. Photochem. Photobiol. Sci. 13, 1730–1740.

Cullity, B.D., 1972. Introduction to Magnetic Materials. Addison-Wesley, Philippines.

Dandamudi, S., Campbell, R.B., 2007. The drug loading, cytotoxicity and tumor vascular targeting characteristics of magnetite in magnetic drug targeting. Biomaterials 28, 4673–4683.

De Cuyper, M., Joniau, M., 1988. Magnetoliposomes: formation and structural characterization. Eur. Biophys. J. 15, 311–319.

Deraz, N.M., Alarifi, A., 2012. Controlled synthesis, physicochemical and magnetic properties of nano-crystalline Mn ferrite system. Int. J. Electrochem. Sci. 7, 5534–5543.

Ding, H., Sagar, V., Agudelo, M., Pilakka-Kanthikeel, S., Atluri, V.S.R., Raymond, A., et al., 2014. Enhanced blood–brain barrier transmigration using a novel transferrin-embedded fluorescent magnetoliposome nanoformulation. Nanotechnology 25, 55–101.

Elmi, M.M., Sarbolouki, M.N., 2001. A simple method for preparation of immunomagnetic liposomes. Int. J. Pharm 215, 45–50.

Escalona, M.M., Sáez-Fernández, E., Prados, J.C., Melguizo, C., Arias, J.L., 2016. Magnetic solid lipid nanoparticles in hyperthermia against colon cancer. Int. J. Pharm. 504, 11–19.

Estelrich, J., Escribano, E., Queralt, J., Busquets, M.A., 2015. Iron oxide nanoparticles for magnetically-guided and magnetically-responsive drug delivery. Int. J. Mol. Sci. 16, 8070–8101.

Fernández-Remolar, D.C., 2014. Iron oxides, hydroxides and oxy-hydroxides. Encyclopedia of Astrobiology. Springer, Berlin, pp. 1268–1270.

Floris, A., Ardu, A., Musinu, A., Piccaluga, G., Fadda, A.M., Sinico, C., 2011. SPION@liposomes hybrid nanoarchitectures with high density SPION association. Soft Matter 7, 6239–6247.

García-Jimeno, S., Escribano, E., Queralt, J., Estelrich, J., 2011. Magnetoliposomes prepared by reverse-phase followed by sequential extrusion: characterization and possibilities in the treatment of inflammation. Int. J. Pharm. 405, 181–187.

Gharagozlou, M., 2011. Influence of calcination temperature on structural and magnetic properties of nanocomposites formed by Co-ferrite dispersed in sol-gel silica matrix using tetrakis(2-hydroxyethyl) orthosilicate as precursor. Chem. Cent. J. 5, 19–26.

Gilchrist, R.K., Medal, R., Shorey, W.D., Hanselman, R.C., Parrott, J.C., Taylor, C.B., 1957. Selective inductive heating of lymph nodes. Ann. Surg. 146, 596–606.

Goodwin, S., Peterson, C., Hoh, C., Bittner, C., 1999. Targeting and retention of magnetic targeted carriers (MTCs) enhancing intra-arterial chemotherapy. J. Magn. Magn. Mater. 194, 132–139.

Gordon, R.T., Hines, J.R., Gordon, D., 1979. Intracellular hyperthermia. A biophysical approach to cancer treatment via intracellular temperature and biophysical alterations. Med. Hypothesis 5, 83–102.

Gregoriadis, G., 1995. Engineering liposomes for drug delivery: progress and problems. Trends Biotechnol. 13, 527–537.

Gribanov, N.M., Bibik, E.E., Buzunov, O.V., Naumov, V.N.J., 1990. Physicochemical regularities of obtaining highly dispersed magnetite by the method of chemical condensation. Magn. Magn. Mater. 85, 7–10.

Gupta, A.K., Wells, S., 2004. Surface-modified superparamagnetic nanoparticles for drug delivery: preparation, characterization, and cytotoxicity studies. IEEE Trans. Nanobiosci. 3, 66–73.

Hafez, I.M., Ansell, S., Cullis, P.R., 2000. Tunable pH-sensitive liposomes composed of mixtures of cationic and anionic lipids. Biophys. J. 79, 1438–1446.

Hardiansyah, A., Huang, L.-Y., Yang, M.-C., Liu, T.-Y., Tsai, S.C., Yang, C.-Y., et al., 2014. Magnetic liposomes for colorectal cancer cells therapy by high-frequency magnetic field treatment. Nanoscale Res. Lett. 9, 497.

Hergt, R., Dutz, S., 2007. Magnetic particle hyperthermia – biophysical limitations of a visionary tumour therapy. J. Magn. Magn. Mater. 311, 187–192.

Hirazawa, H., Kusamoto, S., Aono, H., Naohara, T., Mori, K., Hattori, Y., et al., 2008. Preparation of fine $Mg_{1-X}Ca_XFe_2O_4$ powder using reverse coprecipitation method for thermal coagulation therapy in an AC magnetic field. J. Alloys Compd. 4, 467–473.

Hu, K., Li, J., Shen, Y., Lu, W., Gao, X., Zhang, Q., et al., 2009. Lactoferrin-conjugated PEG-PLA nanoparticles with improved brain delivery: in vitro and in vivo evaluations. J. Control. Release 134, 55–61.

Huang, D.M., Chung, T.H., Hung, Y., Lu, F., Wu, S.-H., Mou, C.Y., et al., 2008. Internalization of mesoporous silica nanoparticles induces transient but not sufficient osteogenic signals in human mesenchymal stem cells. Toxicol. Appl. Pharmacol. 231, 208–215.

Illés, E., Szekeres, M., Kupcsika, E., Tótha, I.Y., Farkas, K., Jedlovszky-Hajdúa, A., et al., 2014. PEGylation of surfacted magnetite core–shell nanoparticles for biomedical application. Colloids Surf. A: Physicochem. Eng. Aspects 460, 429–440.

Indira, T.K., Lakshmi, P.K., 2010. Magnetic nanoparticles – a review. Int. J. Pharm. Sci. Nanotechnol. 3, 1035–1042.

Inouye, K., Endo, R., Otsuka, Y., Miyashiro, K., Kaneko, K., Ishikawa, T., 1982. Oxygenation of ferrous-ions in reversed micelle and reversed micro-emulsion. J. Phys. Chem. 86, 1465–1469.

Issels, R.D., 2008. Hyperthermia adds to chemotherapy. Eur. J. Cancer 44, 2546–2554.

Itoh, Y., Yamada, Y., Kazaoka, Y., Ishiguchi, T., Honda, N., 2010. Combination of chemotherapy and mild hyperthermia enhances the anti-tumor effects of cisplatin and adriamycin in human bladder cancer T24 cells in vitro. Exp. Ther. Med. 1, 319–323.

Jain, S., Mishra, V., Singh, P., Dubey, P.K., Saraf, D.K., Vyas, S.P., 2003. RGD-anchored magnetic liposomes for monocytes/neutrophils-mediated brain targeting. Int. J. Pharm. 261, 43–55.

Jolivet, J.P., Chaeneac, C., 2002. Synthesis of iron oxide-based magnetic nanomaterials and composites. C. R. Chim. 5, 659–664.

Jolivet, J.P., Vassiere, L., Chaeneac, C., Tronc, E., 1997. Precipitation of spinel iron oxide: nanoparticle size control. Mater. Res. Symp. Proc. 432, 145.

Jolivet, J.P., Froidefond, C., Pottier, A., Chaeneac, C., Cassaignon, S., Tronc, E., et al., 2014. Size tailoring of oxide nanoparticles by precipitation in aqueous medium. A semi-quantitative modelling. Mater. Chem. 14, 3281–3288.

Juliano, R.L., 1981. Liposomes as a drug delivery system. Trends Pharmacol. Sci. 2, 39–42.

Kanagesan, S., Hashim, M., Tamilselvan, S., Alitheen, N.B., Ismail, I., Bahmanrokh, G., 2013. Cytotoxic effect of nanocrystalline $MgFe_2O_4$ particles for cancer cure. J. Nanomater. 2013, 865024–865032.

Kaur, N., Kaur, M., 2014. Comparative studies on impact of synthesis methods on structural and magnetic properties of magnesium ferrite nanoparticles. Process. Appl. Ceram. 8, 137–143.

Khanna, L., Verma, N.K., 2013a. Size-dependent magnetic properties of calcium ferrite nanoparticles. J. Magn. Magn. Mater. 336, 1–7.

Khanna, L., Verma, N.K., 2013b. Synthesis, characterization and in vitro cytotoxicity study of calcium ferrite nanoparticles. Mater. Sci. Semicond. Process. 16, 1842–1848.

Kim, T., Momin, E., Choi, J., Kim, T., Momin, E., Choi, J., et al., 2011. Mesoporous silica-coated hollow manganese oxide nanoparticles as positive T_1 contrast agents for labeling and MRI tracking of adipose-derived mesenchymal stem cells. J. Am. Chem. Soc. 133, 2955–2961.

Kobayashi, T., 2011. Cancer hyperthermia using magnetic nanoparticles. Biotechnol. J. 6, 1342–1347.

Kulshrestha, P., Gogoi, M., Bahadur, D., Banerjee, R., 2012. In vitro application of paclitaxel loaded magnetoliposomes for combined chemotherapy and hyperthermia. Colloids Surf. B 96, 1–7.

Kumar, S., 2013. Magnetic nanoparticles-based biomedical and bioanalytical applications. J. Nanomed. Nanotechol. 4, 130–132.

Kuznetsov, A.A., Harutyunyan, A.R., Dobrinsky, E.K., 1997. Scientific and Clinical Applications of Magnetic Carriers. Plenum Press, New York.

Kuznetsov, A.A., Filippov, V.I., Kuznetsov, O.A., Gerlivanov, V.G., Dobrinsky, E.K., Malashin, S.I., 1999. New ferro-carbon adsorbents for magnetically guided transport of anti-cancer drugs. J. Magn. Magn. Mater. 194, 22–30.

Lai, J.C.K., Lai, M.B., Jandhyam, S., 2008. Exposure to titanium dioxide and other metallic oxide nanoparticles induces cytotoxicity on human neural cells and fibroblasts. Int. J. Nanomedicine 3, 533–545.

Laurent, S., Forge, D., Port, M., Roch, A., Robic, C., Vander, E., et al., 2008. Magnetic iron oxide nanoparticles: synthesis, stabilization, vectorization, physicochemical characterizations, and biological applications. Chem. Rev. 108, 2064–2110.

Laurent, S., Dutz, S., Häfeli, U.O., Mahhmoudi, M., 2011. Magnetic fluid hyperthermia: focus on superparamagnetic iron oxide nanoparticles. Adv. Colloid Interface Sci. 166, 8–23.

Law, W.-C., Yong, K.-T., Roy, I., Xu, G., Ding, H., Bergey, E.J., 2008. Optically and magnetically doped organically modified silica nanoparticles as efficient magnetically guided biomarkers for two-photon imaging of live cancer cells. J. Phys. Chem. C 112, 7972–7977.

Lee, Y., Lee, J., Bae, C.J., Park, J.G., Noh, H.J., 2005. Largescale synthesis of uniform and crystalline magnetite nanoparticles using reverse micelles as nanoreactors under reflux conditions. Adv. Funct. Mater. 15, 503–509.

Li, F., Sun, J., Zhu, H., Wen, X., Lin, C., Shi, D., 2011. Preparation and characterization novel polymer-coated magnetic nanoparticles as carriers for doxorubicin. Colloids Surf. B: Biointerfaces 88, 58–62.

Li, Z., Wang, S.X., Sun, Q., Zhao, H.L., Lei, H., Lan, M.B., et al., 2013. Ultrasmall manganese ferrite nanoparticles as positive contrast agent for magnetic resonance imaging. Adv. Healthcare Mater. 2, 958–964.

Li-Ying, Z., Yong-Hua, D., Ling, Z., Hong-Chen, G., 2010. Magnetic behavior and heating effect of Fe_3O_4 ferrofluids composed of monodisperse nanoparticles. Chin. Phys. Lett. 24, 483–486.

Lu, W., Shen, Y., Xie, A., Zhang, W., 2010. Green synthesis and characterization of superparamagnetic Fe_3O_4 nanoparticles. J. Magn. Magn. Mater. 322, 1828–1833.

Lubbe, A.S., Bergemann, C., Brock, J., McClure, D.G., 1999. Physiological aspects in magnetic drug-targeting. J. Magn. Magn. Mater. 194, 149–155.

Maaz, K., Karim, S., Mumtaz, A., Hasanain, S.K., Liu, J., Duan, J.L., 2009. Synthesis and magnetic characterization of nickel ferrite nanoparticles prepared by coprecipitation route. J. Magn. Magn. Mater. 321, 1838–1842.

Maehara, T., Konishi, K., Kamimori, T., Aono, H., Hirazawa, H., Naohara, T., 2005. Selection of ferrite powder for thermal coagulation therapy with alternating magnetic field. J. Mater. Sci. 40, 135–138.

Maensiri, S., Sangmanee, M., Wiengmoon, A., 2009. Magnesium ferrite ($MgFe_2O_4$) nanostructures fabricated by electrospinning. Nanoscale Res. Lett. 4, 221–228.

Mahmoudi, M., Sant, S., Wang, B., Laurent, S., Sen, T., 2011. Superparamagnetic iron oxide nanoparticles (SPIONs): development, surface modification and applications in chemotherapy. Adv. Drug Deliv. Rev. 63, 24–46.

Malik, R., Annapoorni, S., Lamba, S., Reddy, V.R., Gupta, A., Sharma, P., et al., 2010. Mossbauer and magnetic studies in nickel ferrite nanoparticles: effect of size distribution. J. Magn. Magn. Mater. 322, 3742–3747.

Markides, H., Rotherham, M., El Haj, A.J., 2012. Biocompatibility and toxicity of magnetic nanoparticles in regenerative medicine. J. Nanomater. 2012, 1–11.

Massart, R., Cabuil, V., 1987. Effect of some parameters on the formation of colloidal magnetite in alkaline-medium-yield and particles-size control. J. Chim. Phys. 84, 967–973.

Mathew, D.S., Juang, R.-S., 2007. An overview of the structure and magnetism of spinel ferrite nanoparticles and their synthesis in microemulsions. Chem. Eng. J. 129, 51–65.

Mathieu, J.B., Martel, S., 2010. Steering of aggregating magnetic microparticles using propulsion gradients coils in an MRI scanner. Magn. Reson. Med. 63, 1336–1345.

Medeiros, S.F., Santos, A.M., Fessi, H., Elaissari, A., 2011. Stimuli-responsive magnetic particles for biomedical applications. Int. J. Pharm. 403, 139–161.

Meledandri, C.J., Ninjbadgar, T., Brougham, D.F., 2011. Size controlled magnetoliposomes with tunable magnetic resonance relaxation enhancements. J. Mater. Chem. 21, 214–222.

Mezei, M., Gulasekharam, V., 1982. Liposomes – a selective drug delivery system for the topical route of administration: gel dosage form. J. Pharm. Pharmacol. 34, 473–474.

Mishra, B., Patel, B.B., Tiwari, S., 2010. Colloidal nanocarriers: a review on formulation technology, types and applications toward targeted drug delivery. Nanomed. Nanotechnol. 6, 9–24.

Mitsumata, T., Honda, A., Kanazawa, H., Kawai, M., 2012. Magnetically tunable elasticity for magnetic hydrogels consisting of carrageenan and carbonyl iron particles. J. Phys. Chem. B 116, 12341–12348.

Monnier, C.A., Burnand, D., Rothen-Rutishauser, B., Lattuada, M., Petri-Fink, A., 2014. Magnetoliposomes: opportunities and challenges. Eur. J. Nanomed. 6, 201–215.

Muller, B.W., Muller, R.H., 1984. Particle-size distributions and particle-size alterations in microemulsions. J. Pharm. Sci. 73, 919–922.

Murugesan, C., Chandrasekaran, G., 2015. Enhanced electrical and magnetic properties of annealed magnesium ferrite nanoparticles. J. Supercond. Nov. Magn. 28, 3607–3615.

Nappini, S., Bombelli, F.B., Bonini, M., Norden, B., Baglioni, P., 2010. Magnetoliposomes for controlled drug release in the presence of lowfrequency magnetic field. Soft Matter. 6, 154–162.

Nejati, K., Zabihi, R., 2012. Preparation and magnetic properties of nano size nickel ferrite particles using hydrothermal method. Chem. Cent. J. 23, 1–6.

Nuytten, N., Hakimhashemi, M., Ysenbaert, T., Defour, L., Trekker, J., Soenen, S.J. H., et al., 2010. PEGylated lipids impede the lateral diffusion of adsorbed proteins at the surface of (magneto)liposomes. Colloids Surf. B 80, 227–231.

Ochekpe, N.A., Olorunfemi, P.O., Ngwuluka, N.C., 2009. Nanotechnology and drug delivery part 1: background and applications. Trop. J. Pharm. Res. 8, 265–274.

Pereira, C., Pereira, A.M., Fernandes, C., Rocha, M., Mendes, R., Garcia, M.P.F., et al., 2012. Superparamagnetic MFe_2O_4 (M = Fe, Co, Mn) nanoparticles: tuning the particle size and magnetic properties through a novel one-step coprecipitation route. Chem. Mater. 24, 1496–1504.

Perez, J.A.L., Quintela, M.A.L., Mira, J., Rivas, J., Charles, S.W., 1997. Advances in the preparation of magnetic nanoparticles by the microemulsion method. J. Phys. Chem. B 101, 8045–8047.

Perry, M., 2001. The Chemotherapy Source Book, third ed. Lippincott Williams & Wilkins, Philadelphia.

Poste, G., Cucana, C., Raz, A., Bugelski, P., Kirsh, R., Fidler, I.J., 1982. Analysis of the fate of systemically administered liposomes and implications for their use in drug delivery. Cancer Res. 24, 1412–1422.

Pouponneau, P., Savadogo, O., Napporn, T., Yahia, L., Martel, S., 2010. Corrosion study of iron-cobalt alloys for MRI-based propulsion embedded in untethered microdevices operating in the vascular network. J. Biomater. Mater. Res. B: Appl. Biomater. 93, 203–211.

Pradhan, P., Giri, J., Banerjee, R., Bellare, J., Bahadur, D., 2007. Preparation and characterization of manganese ferrite-based magnetic liposomes for hyperthermia treatment of cancer. J. Magn. Magn. Mater. 311, 208–215.

Pradhan, P., Giri, J., Reiken, F., Koch, C., Mykhaylyk, O., Döblinger, M., et al., 2010. Targeted temperature sensitive magnetic liposomes for thermo-chemotherapy. J. Control. Release 142, 108–121.

Queiroz, M.-J.R.P., Calhelha, R.C., Vale-Silva, L., Pinto, E., Nascimento, M.S.-J., 2010. Novel [6-(hetero)arylamino]thieno[3,2-*b*]pyridines: synthesis and antitumoral activities. Eur. J. Med. Chem. 45, 5732–5738.

Rafique, M.Y., Li-Qing, P., Javed, Q., Iqbal, M.Z., Hong-Mei, Q., Farooq, M.H., et al., 2013. Growth of monodisperse nanospheres of $MnFe_2O_4$ with enhanced magnetic and optical properties. Chin. Phys. B 22, 107101–107107.

Rao, W., Deng, Z.-S., Liu, J., 2010. A review of hyperthermia combined with radiotherapy/chemotherapy on malignant tumors. Crit. Rev. Biomed. Eng. 38, 101–116.

Reszka, R., Beck, P., Fichtner, I., Hentschel, M., Richter, J., Kreuter, J., 1997. Body distribution of free liposomal and nanoparticle associated mitoxantrone in B16-melanoma-bearing mice. J. Pharmacol. Exp. Ther. 280, 232–237.

Rodrigues, A.R.O., Gomes, I.T., Almeida, B.G., Araújo, J.P., Castanheira, E.M.S., Coutinho, P.J.G., 2014. Magnetoliposomes based on nickel/silica core/shell nanoparticles: synthesis and characterization. Mater. Chem. Phys. 148, 978–987.

Rodrigues, A.R.O., Gomes, I.T., Almeida, B.G., Araújo, J.P., Castanheira, E.M.S., Coutinho, P.J.G., 2015. Magnetic liposomes based on nickel ferrite nanoparticles for biomedical applications. Phys. Chem. Chem. Phys. 17, 18011–18021.

Rodrigues, A.R.O., Ramos, J.M.F., Gomes, I.T., Almeida, B.G., Araújo, J.P., Queiroz, M.J.R.P., et al., 2016. Magnetoliposomes based on manganese ferrite nanoparticles as nanocarriers for antitumor drugs. RSC Adv. 6, 17302–17313.

Rodrigues, A.R.O., Almeida, B.G., Rodrigues, J.M., Queiroz, M.J.R.P., Calhelha, R. C., Ferreira, I.C.F.R., et al., 2017. Magnetoliposomes as carriers for promising antitumor thieno[3,2-*b*]pyridine-7-arylamines: photophysical and biological studies. RSC Adv. 7, 15352–15361.

Saldívar-Ramírez, M.M.G., Sánchez-Torres, C.G., Cortés-Hernández, D.A., Escobedo-Bocardo, J.C., Almanza-Robles, J.M., Larson, A., et al., 2014. Study on the efficiency of nanosized magnetite and mixed ferrites in magnetic hyperthermia. J. Mater. Sci: Mater. Med. 25, 2229–2236.

Sato, K., Watanabe, Y., Horiuchi, A., Yukumi, S., Doi, T., Yoshida, M., 2008. Feasibility of new heating method of hepatic parenchyma using a sintered $MgFe_2O_4$ needle under an alternating magnetic field. J. Surg. Res. 146, 110–116.

Sattler, K.D., 2010. Handbook of Nanophysics: Principles and Methods. CCR Press, Boca Raton.

Schulz, D.L., Sailer, R.A., Caruso, A.N., 2009. Superparamagnetic transition metal iron oxygen nanoparticles. US Patent No. 0194733.

Sharifi, I., Shokrollahi, H., Amiri, S., 2012. Ferrite-based magnetic nanofluids used in hyperthermia applications. J. Magn. Magn. Mater. 424, 903–915.

Shubitidze, F., Kekalo, K., Stigliano, R., Baker, I., 2015. Magnetic nanoparticles with high specific absorption rate of electromagnetic energy at low field strength for hyperthermia therapy. J. Appl. Phys. 117, 94302–94314.

Sivakumar, P., Ramesh, R., Ramanand, A., Ponnusamy, S., Muthamizhxhelvan, C., 2011a. Synthesis and characterization of $NiFe_2O_4$ nanosheet via polymer assisted coprecipitation method. Mater. Lett. 65, 483–485.

Sivakumar, P., Ramesh, R., Ramanand, A., Ponnusamy, S., Muthamizhchelvan, C., 2011b. Preparation and properties of nickel ferrite ($NiFe_2O_4$) nanoparticles via sol–gel auto-combustion method. Mater. Res. Bull. 46, 2204–2207.

Sjogren, C.E., Johansson, C., Naevestad, A., Sontum, P.C., BrileySaebo, K., 1997. Crystal size and properties of superparamagnetic iron oxide (SPIO) particles. Magn. Reson. Imaging 15, 55–67.

Sounderya, N., Zhang, Y., 2008. Use of core/shell structured nanoparticles for biomedical applications. Recent. Pat. Biomed. Eng. 1, 34–42.

Sulaiman, N.H., Ghazali, M.J., Majlis, B.Y., Yunas, J., Razalia, M., 2015. Superparamagnetic calcium ferrite nanoparticles synthesized using a simple sol–gel method. Bio-Med. Mater. Eng. 26, S103–S110.

Sulaiman, N.H., Ghazali, M.J., Majlis, B.Y., Yunas, J., Razali, M., 2016. Influence of polyvinylalcohol on the size of calcium ferrite nanoparticles synthesized using a sol–gel technique. In: International Conference for Innovation in Biomedical Engineering and Life Sciences, vol. 56, pp. 198–202.

Teja, A.S., Koh, P.-Y., 2009. School synthesis, properties, and applications of magnetic iron oxide nanoparticles. Prog. Cryst. Growth Charac. Mater. 55, 22–45.

Thong-On, B., Rutnakornpituk, B., Wichai, U., Rutnakornpituk, M., 2012. Magnetite nanoparticle coated with amphiphilic bilayer surfactant of polysiloxane and poly (poly(ethylene glycol) methacrylate). J. Nanopart. Res. 14, 953–965.

Tomitaka, A., Hirukawa, A., Yamada, T., Morishit, S., Takemura, Y., 2009. Biocompatibility of various ferrite nanoparticles evaluated by in vitro cytotoxicity assays using HeLa cells. J. Magn. Magn. Mater. 321, 1482–1484.

Toniolo, C., Crisma, M., Formaggio, F., Peggion, C., Monaco, V., Goulard, C., et al., 1996. Effect of N-acyl chain length on the membrane-modifying properties of synthetic analogs of the lipopeptaibol trichogin GA IV. J. Am. Chem. Soc. 118, 4952–4958.

Tromsdorf, U.I., Bigall, N.C., Kaul, M.G., Bruns, O.T., Nikolic, M.S., Mollwitz, B., et al., 2007. Size and surface effects on the MRI relaxivity of manganese ferrite nanoparticle contrast agents. Nano Lett. 7, 2422–2427.

van der Veldt, A.A.M., Hendrikse, N.H., Smit, E.F., Mooijer, M.P.J., Rijnders, A.Y., Gerritsen, W.R., et al., 2010. Biodistribution and radiation dosimetry of 11C-labelled docetaxel in cancer patients. Eur. J. Nucl. Med. Mol. Imaging 37, 1950–1958.

Veiseh, O., Gunn, J.W., Zhang, M., 2010. Design and fabrication of magnetic nanoparticles for targeted drug delivery and imaging. Adv. Drug Deliv. Rev. 62, 284–304.

Vestal, C.R., Zhang, J.Z., 2004. Magnetic spinel ferrite nanoparticles from microemulsions. Int. J. Nanotechnol. 1, 240–263.
Wan, Y., Xiong, G., Luo, H., He, F., Huang, Y., Zhou, X., 2008. Preparation and characterization of a new biomedical magnesium–calcium alloy. Mater. Des. 29, 2034–2037.
Weinmann, H.-J., Ebert, W., Misselwitz, B., Schmitt-Willich, H., 2003. Tissue-specific MR contrast agents. Eur. J. Radiol. 46, 33–44.
Yanase, M., Shinkai, M., Honda, H., Wakabayashi, T., 1998. Antitumor immunity induction by intracellular hyperthermia using magnetite cationic liposomes. Jpn. J. Cancer Res. 89, 775–782.
Zhang, J.Q., Zhang, Z.R., Yang, H., Tan, Q.Y., Qin, Q.Y., Qiu, X.L., 2005. Lyophilized paclitaxel magnetoliposomes as a potential drug delivery system for breast carcinoma via parenteral administration: in vitro and in vivo studies. Pharm. Res. 22, 573–583.
Zhang, S., Niu, H., Zhang, Y., Liu, J., Shia, Y., Zhang, X., et al., 2012. Biocompatible phosphatidylcholine bilayer coated on magnetic nanoparticles and their application in the extraction of several polycyclic aromatic hydrocarbons from environmental water and milk samples. J. Chromatogr. A 1238, 38–45.
Zhao, M., Chang, J., Fu, X., Liang, C., Liang, S., Yan, R., et al., 2012. Nano-sized cationic polymeric magnetic liposomes significantly improve drug delivery to the brain in rats. J. Drug Deliv. 20, 416–421.
Zipare, K., Dhumal, J., Bandgar, S., Mathe, V., Shahane, G., 2015. Superparamagnetic manganese ferrite nanoparticles: synthesis and magnetic properties. J. Nanosci. Nanotechnol. 1, 178–182.

FURTHER READING

Cullity, B.D., Graham, C.D., 1999. Introduction to Magnetic Materials. John Wiley & Sons Inc, New Jersey.
Frey, N.A., Peng, S., Cheng, K., Sun, S., 2009. Magnetic nanoparticles: synthesis, functionalization, and applications in bioimaging and magnetic energy storage. Chem. Soc. Rev. 38, 2532–2542.
Illés, E., Tombácz, E., Szekeres, M., Tóth, I.Y., Szabó, Á., Iván, B., 2015. Novel carboxylated PEG-coating on magnetite nanoparticles designed for biomedical applications. J. Magn. Magn. Mater. 380, 132–139.
Jordan, A., Scholz, R., Wust, P., Schirra, H., Thomas, S., Schmidt, H., 1999. Endocytosis of dextran and silan-coated magnetite nanoparticles and the effect of intracellular hyperthermia on human mammary carcinoma cells in vitro. J. Magn. Magn. Mater. 194, 185–196.
Jun, Y.W., Huh, Y.M., Choi, J.S., Lee, J.H., Song, H.T., 2005. Nanoscale size effect of magnetic nanocrystals and their utilization for cancer diagnosis via magnetic resonance imaging. J. Am. Chem. Soc. 127, 5732–5733.